

DE-EE0003585

Innovative Phase Change Thermal Energy Storage Solution for Baseload Power
Infinia Corporation

Phase 1 Final Report

Project Title: Innovative Phase Change Thermal Energy Storage Solution for Baseload Power

Project Period: 09/27/10 – 12/12/14

Budget Period: Phase 1, 09/27/10 – 4/30/13

Budget Period Budget: \$999,327

Submission Date: 5/15/13

Recipient: Infinia Corporation

Address: 300 West 12th Street
Ogden, UT 84404

Award Number: DE-EE0003585

Project Team: Barry Penswick, Consultant
Temple University

Contacts: Songgang Qiu, Ph.D.
Vice President Research and Development
Phone: 509-308-2702
Email: sqiu@infiniacorp.com

Innovative Phase Change Thermal Energy Storage Solution for Baseload Power
Infinia Corporation

Executive Summary: The primary purpose of this project is to develop and validate an innovative, scalable phase change salt thermal energy storage (TES) system that can interface with Infinia's family of free-piston Stirling engines (FPSE). This TES technology is also appropriate for Rankine and Brayton power converters. Solar TES systems based on latent heat of fusion rather than molten salt temperature differences, have many advantages that include up to an order of magnitude higher energy storage density, much higher temperature operation, and elimination of pumped loops for most of Infinia's design options. DOE has funded four different concepts for solar phase change TES, including one other Infinia awarded project using heat pipes to transfer heat to and from the salt. The unique innovation in this project is an integrated TES/pool boiler heat transfer system that is the simplest approach identified to date and arguably has the best potential for minimizing the levelized cost of energy (LCOE). The Phase 1 objectives are to design, build and test a 1-hour TES proof-of-concept lab demonstrator integrated with an Infinia 3 kW Stirling engine, and to conduct a preliminary design of a 12-hour TES on-sun prototype.

Early in Phase I, before starting the design of the lab demonstrator, a decision was made in collaboration with the DOE project monitor to build and test subscale TES units to validate the basic physics and better understand processes during operation. These subscale test modules, which were not in the original project scope, provided valuable data, lessons learned and verification of the proof of concept, but negatively impacted the overall schedule. Three generations of subscale units were developed and tested due to initial subscale design artifacts that compromised results. The Gen 3 unit demonstrated recovery of 2/3 of the stored latent heat (still a far better energy storage density than any known alternative) and provided results that enabled significant improvements in the lab demonstrator, which was tested successfully in December 2012; generating 3.9 kW-h of electrical energy from stored thermal energy. The testing also revealed a need to better understand the complex salt dynamics within the device. To that end, Temple University researchers developed computer simulations, which will serve as the basis for advancing the understanding of how salt behaves in this two-phase system. A high-level heat transport system study for de-coupling the solar receiver from the TES/engine system was conducted. Further Phase I tasks for preliminary system design and LCOE analysis were contingent on results from the lab demonstrator – the testing of which consumed the balance of the schedule, resulting in a minimal effort expended on those tasks.

Innovative Phase Change Thermal Energy Storage Solution for Baseload Power
Infinia Corporation

Table of Contents

Executive Summary: 2

Table of Contents 3

Background: 4

Introduction: 6

 Task 1: TES Lab-Scale Module Design 9

 Task 2: TES Module Lab Demonstration 10

 Task 3: Receiver/Heat Transport System 10

 Task 4: System Preliminary Design 10

 Task 5: Cost and Capacity Factor Analysis..... 10

 Task 6: Project Management and Reporting..... 10

 Critical Milestone Phase 1 Go/No-Go Criteria..... 10

 Critical Milestones for Phase 1 11

 DOE Phase 1 Feasibility Study Evaluation Criteria (Go/No-Go Decision) 11

 Interim Critical Milestones..... 12

Project Results and Discussion: 12

 Task 1: TES Lab-Scale Module Design 12

 Subscale TES Evaluation Module Design 13

 Lab-scale TES Module Design 22

 Task 2: TES Module Lab Demonstration 24

 Task 3: Receiver/Heat Transport System (HTS)..... 36

 Task 4: System Preliminary Design 37

 Task 5: Cost and Capacity Factor Analysis..... 39

 Model Description 39

 Model Results 39

Conclusions:..... 41

Budget and Schedule:..... 42

Path Forward:..... 42

References:..... 49

Appendix A: Temple University Report 51

Innovative Phase Change Thermal Energy Storage Solution for Baseload Power Infinia Corporation

Background: CSP systems can be categorized under four technology families: parabolic troughs, power towers (a.k.a. “central receiver systems” – CRS), linear Fresnel reflectors, and parabolic dishes/engines. These technologies are further delineated according to how they focus and receive the sun [IEA, 2012].

A technological comparison of these four CSP systems is shown in Table 1 [IRENA, 2012]. From this table, it is observed that parabolic dishes demonstrate the greatest efficiencies, due to their capability of operating at much higher temperatures, and their much more simplistic designs. However, parabolic dish energy storage potential is offset by its relative immaturity compared to other technologies.

Table 1: CSP Technology Comparison

	Parabolic Trough	Solar Tower	Linear Fresnel	Dish Stirling
Typical capacity (MW)	10-300	10-200	10-200	0.01-0.025
Maturity of technology*	Commercially proven	Commercially proven	Commercially proven	Commercial Demonstration projects
Maturity of TES technology*	Commercially available	Commercially available	Commercially available in 2013	Possible, but not proven
Key technology providers	Abengoa Solar, SolarMillenium, Sener Group, Acciona, Siemens, NextEra, ACS, SAMCA, etc.	Abengoa Solar, BrightSource, Energy, eSolar, SolarReserve, Torresol	Novatec Solar, Areva	
Technology development risk	Low	Medium	Medium	Medium
Operating temperature (°C)	350-550	250-565	390	550-750
Plant peak efficiency (%)	14-20	23-35	18	30
Annual solar-to-electricity efficiency (%)	11-16	7-20	13	12-25
Annual capacity factor (%)	25-28 (no TES) 29-43 (7h TES)	55 (10h TES)	22-24	25-28
Collector concentration	70-80 suns	>1,000 suns	>60 suns (depends on secondary reflector)	>1,300 suns
Receiver/absorber	Absorber attached to collector, moves with collector, complex design	External surface or cavity receiver, fixed	Fixed absorber, no evacuation secondary reflector	Absorber attached to collector, moves with collector
Storage system	Indirect two-tank molten salt at 380°C (dT=100K) or Direct two-tank molten salt at 550°C (dT=300K)	Direct two-tank molten salt at 550°C (dT=300K)	Short-term pressurized steam storage (<10 min)	No storage for Stirling dish, PCM storage under development
Hybridisation	Yes and direct	Yes	Yes, direct (steam boiler)	Not planned
Grid stability	Medium to high (TES or hybridisation)	High (large TES)	Medium (back-up firing possible)	Low
Cycle	Superheated Rankine steam cycle	Superheated Rankine steam cycle	Saturated Rankine steam cycle	Stirling
Steam conditions (°C/bar)	380 to 540/100	540/100 to 160	260/50	n.a.
Maximum slope of solar field (%)	<1-2	<2-4	<4	10%>
Water requirement (m ³ /MWh)	3 (wet cooling) 0.3 (dry cooling)	2-3 (wet cooling) 0.25 (dry cooling)	3 (wet cooling) 0.2 (dry cooling)	0.05-0.1 (mirror washing)
Application type	On-grid	On-grid	On-grid	On-grid/Off-grid
Suitability for air cooling	Low to good	Good	Low	Best

Sources: IRENA, 2012 as referenced from Fichtner, 2010 (*updated for 2012 advances in technology)

Innovative Phase Change Thermal Energy Storage Solution for Baseload Power
Infinia Corporation

To date, only parabolic troughs, power towers, and linear Fresnel reflectors have commercially incorporated long term (direct or indirect storage using one or two tanks) or short term (pressurized steam storage <10 minutes) TES technology.

More recently, AREVA Solar is collaborating with Sandia National Laboratories to commercially launch its modular Compact Linear Fresnel Reflector (CLFR) for long-term, molten salt storage in 2013 [AREVA, 2012]. Infinia Corporation has begun to develop a scalable 3 kW FPSE with thermal energy storage capabilities using Phase-Change Material (PCM) technology in solar PowerDish™ applications.

In 2010, DOE awarded thirteen projects as part of the Baseload Concentrating Solar Power (CSP) Generation funding opportunity. A large portion of the awarded projects are conducting further research into Sensible Heat Storage (i.e. Abengoa, eSolar, etc.), Thermochemical Heat Storage (i.e. General Atomics) and/or system optimization (i.e. HiTek, PPG, etc.). Infinia's Latent Heat Storage (LHS) application, using innovative phase-change TES Stirling PowerDish™ technology, is a unique line of research similar only to two other awarded projects: Terrafore's and the University of South Florida's (USF's) encapsulated phase-change material (PSM) applications. However, despite the similar use of phase-change material, Infinia's proven, high-temperature FPSE PowerDish™ technology maintains the greatest potential to provide a far more efficient, simplistic, and cost effective thermal energy storage design.

Infinia's 3kW FPSE system was designed to utilize the high temperatures (600-800°C) generated by the Infinia PowerDish™ to store heat in phase-change salts integrated with a liquid metal pool boiler. Heat is then transferred from the boiler directly to the engine heater head where Na vapor condenses, resulting in greatly increased heat transfer rates from the TES boiler to the power block. This high temperature, maintenance-free, hermetically-sealed system not only overcomes the barrier of low thermal conductivity, but also addresses major disadvantages inherent to the other molten salt and PCM system designs. Infinia TES/Stirling system advantages over competitive technologies include those below, with more details in the next section.

- High effective thermal conductivity and heat transfer rates between the TES and power block
- Very high energy density as compared to molten salt systems
- High system efficiency potential >30% (historically much greater all other system technologies)
- Smaller and simpler systems compared to a thermocline or two-tank system

Innovative Phase Change Thermal Energy Storage Solution for Baseload Power
Infinia Corporation

- Lower costs due to reduced HTF and elimination of pumped loops
- No maintenance

Currently, no Stirling dish systems possess TES capabilities. This pioneered application of PCM for thermal energy storage demonstrates that a Stirling TES system poses numerous advantages over competing technologies. Reduced HTF and vessel volumes, a simplified transfer network, and record-holding efficiency levels (as high as 31.25%) support the Stirling PowerDish™ PCM TES system's potential to meet the DOE SunShot goal of \$0.06/kWh [Andraka et al, 2012].

Introduction: Infinia introduced the concept of phase change salt TES for dish Stirling applications in 2008 [Infinia, 2008]. A recent Sandia report [Andraka et al, 2012] assessed the feasibility of a 25 kW dish Stirling system with 6 hours of phase-change TES and concluded that it is likely practical, has leapfrog potential, can have "... an exergetic efficiency above that of current technologies", and has a lower system LCOE than dish Stirling systems without TES. The Sandia concept uses heat pipes to transfer heat to and from the TES material in virtually the same manner as Infinia has successfully demonstrated on a Navy SBIR project. Infinia also used a variant of that approach in its heat pipe phase change DOE TES project, which had limited success due to the temperature drop across salt frozen on the heat pipes during heat extraction. Sandia proposes to use phase change copper-silicon metal eutectic rather than salt eutectic to greatly increase TES thermal conductivity, which reduces a selected combination of this heat extraction temperature drop and the number of relatively costly heat pipes required. This is an intriguing concept with excellent potential, but long-term stability of the metal eutectic and its compatibility with containment materials are significant unknowns. The extensive array of Na heat pipes is also a serious cost concern.

This current project has many advantages over any alternative approach, some of which were highlighted above. The bullet list below summarizes all advantages.

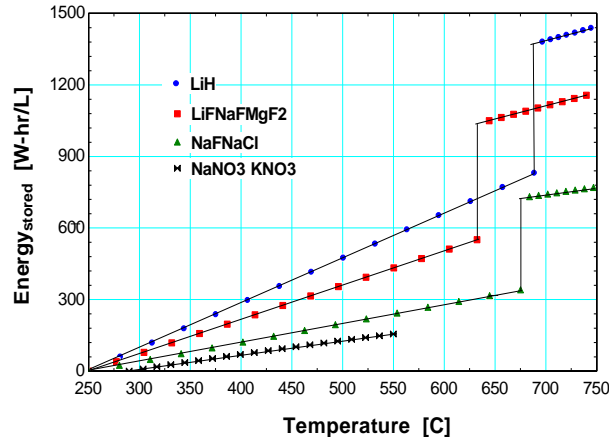
- Unique integral TES/pool boiler approach uses latent heat storage and can adapt to any type of power conversion unit from a few kW to tens or hundreds of MW
- Phase change latent heat TES has very high energy density
- Eliminates the need for heat pipes to reduce cost and complexity
- Pure or eutectic salts can be selected for virtually any melt temperature from under 300 C to over 1300 C
- NaF/NaCl eutectic was selected for very low cost with excellent 680 C melt point

Innovative Phase Change Thermal Energy Storage Solution for Baseload Power
Infinia Corporation

- Engine extracts heat near melt point to always operate at optimum temperature
- Hermetically sealed salt module is maintenance free
- No high temperature pumps or swivel joints needed
- Salt freezing is a non-issue that occurs during normal operation
- Infinia LiF/NaF test module cycled through three 652°C melt/freeze cycles per day for over 4 years with negligible impact on stainless steel containment vessel

The major weight and volume advantages of phase-change TES versus molten salt TES are illustrated by the comparisons in Figure 1. The commonly used NaNO₃/KNO₃ molten salt TES is illustrated over its maximum practical operating range of 250°C to 550°C. The NaF/NaCl eutectic is the low cost alternative selected for this project. Lithium salts typically have significantly better energy storage density but they are more expensive. The eutectic noted is one that Infinia and its predecessors primarily used for their artificial heart TES systems from the late 1960's to the early 1990's. LiH is costly, but it has exceptional energy storage density and was successfully demonstrated by Infinia in 2010 for a heat pipe TES system integrated with a 3 kW FPSE for the Navy.

Innovative Phase Change Thermal Energy Storage Solution for Baseload Power
Infinia Corporation



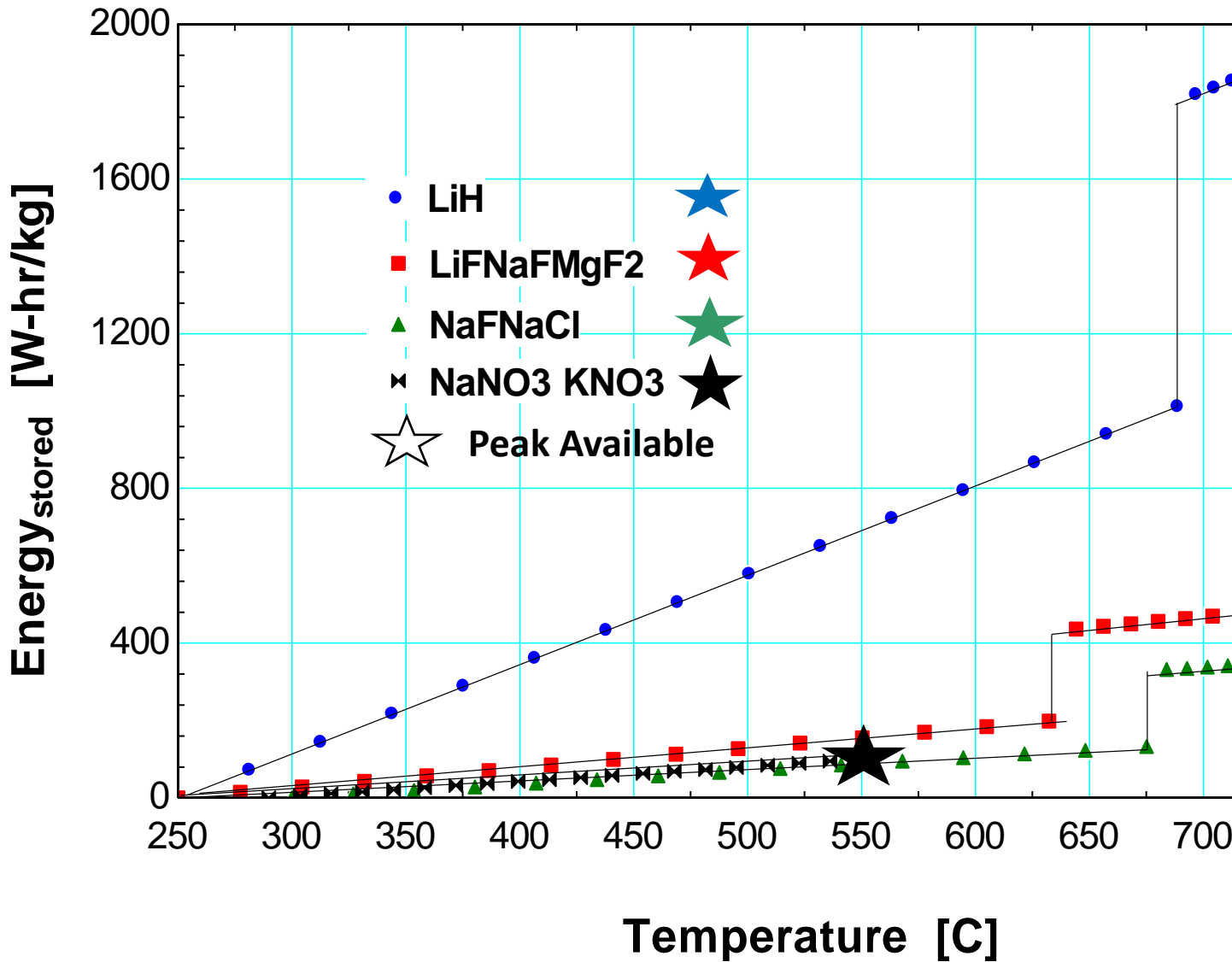


Figure 1, Comparative TES material energy densities by volume (left) and weight (right)

The Phase I Statement of Project Objectives (SOPO) tasks, relevant milestones and go/no go decision points are summarized below.

Task 1: TES Lab-Scale Module Design

Develop complete design of a lab-scale TES module using an innovative in-situ heat transfer mechanism incorporated with an Infinia 3-kW engine. Develop proof of concept subscale module(s) using gas-gap calorimeter or other heat exchanger in lieu of engine to test and evaluate concept functionality.

Innovative Phase Change Thermal Energy Storage Solution for Baseload Power
Infinia Corporation

Task 2: TES Module Lab Demonstration

Infinia will demonstrate the effectiveness of the in-situ heat transfer mechanism as it applies to a solar thermal energy storage device and Stirling engine. At a minimum, the lab demonstration will measure heat distribution as a function of Q into the system, Q out of the system, kW-h effective storage, and temperature deltas.

Task 3: Receiver/Heat Transport System

Infinia will examine many methods of heat transport from the Receiver to the TES and down-select the best design option. Options include a pumped loop heat pipe, Qu Tube, heat pipe, pumped loop NaK/Na, and pumped loop salt. In addition, a new receiver design will be conceptualized that incorporates the selected HTS system. Barry Penswick will be a key resource in developing the HTS system.

Task 4: System Preliminary Design

All design components will be integrated into a preliminary design of a 3-kW dish prototype with 12 hours of thermal storage.

Task 5: Cost and Capacity Factor Analysis

Conduct a manufacturing cost analysis and assess the impact of the proposed TES on the LCOE of 3-kW and 30-kW dish-Stirling CSP systems. The SAM will be modified to allow thermal energy storage for dish-Stirling systems and utilized for the analysis.

Task 6: Project Management and Reporting

Perform necessary reporting and coordination of activities. Reports and other deliverables will be provided in accordance with the Federal Assistance Reporting Checklist following the instructions included therein.

Critical Milestone Phase 1 Go/No-Go Criteria

Key to the development of Infinia's baseload system is the thermal energy storage device. As envisioned, this device is a leap forward beyond Infinia's current effort which utilizes heat pipe networks to move heat into and out of the TES device. Using sodium, *in-situ*, as a heat transport medium, greatly reduces the cost of the TES system, allowing for much larger storage devices and enables capacity factors necessary for baseload power. As such, Infinia views the Phase 1 demonstration of a 1-hour TES device with the proposed innovative architecture as a critical go/no-go step. If the device does not show greater performance over a similar heat piped device (measured ultimately in component cost and associated LCOE impact), it's not clear the project should go forward into Phase 2. If proven, however, to function similarly or substantially

Innovative Phase Change Thermal Energy Storage Solution for Baseload Power
Infinia Corporation

better than a heat pipe enabled device, the potential to realize cost savings at the baseload condition suggests strongly that the project should go into Phase 2 final design.

DOE will make the ultimate decision whether a project will be entitled to proceed. DOE will also verify the economic analysis as part of the go/no go decision.

Critical Milestones for Phase 1

- Demonstration of a 1-hour TES device with the proposed innovative architecture; Integration of design components into a preliminary design of a 3-kW dish demonstration prototype with 12 hours of thermal storage.
- Manufacturing cost analysis and assess the impact of the proposed TES for the 3-kW and 30-kW dish-Stirling CSP systems. A detailed cost analysis, including breakdown of component, material, and labor costs, will be submitted using the SAM model economic assumptions provided. The goal of this cost analysis and assessment is to demonstrate the concepts are applicable and replicable to utility-scale wholesale power generation for 100 MW or greater with a levelized cost of energy (LCOE) of 8 to 9¢/kWh, in real 2009\$, and a capacity factor of 75% (6500 hours per year of operation; at least 85% of electricity from CSP) by 2020.

At the end of Phase 1, the feasibility study and engineering designs will be evaluated in terms of the following minimum criteria, as applicable:

DOE Phase 1 Feasibility Study Evaluation Criteria (Go/No-Go Decision)

- Innovation of the proposed concept or component
- Ability of the concept or component to integrate with a complete CSP system and likelihood of the proposed approach to successfully meet the capacity factor and/or cost (LCOE) goals of project
- Identification and understanding of technical barriers of the proposed concept or component and approach to addressing and evaluating the identified technical barriers
- Description of protocols for evaluating the concept or components
- Environmental impacts of the approach (e.g. amount of water required, physical footprint, hazardous materials utilization, carbon emissions including the net impact from hybridization, etc.)

Innovative Phase Change Thermal Energy Storage Solution for Baseload Power
Infinia Corporation

- Reasonableness of updated Phase 2 and Phase 3 cost proposals and schedules, if necessary
- Capability of the team to develop and execute the project

In late 2011, Infinia requested and received a 10 month, no-cost extension. DOE contract monitors put in place some additional milestones as follows:

Interim Critical Milestones

- Milestone #1 - March 31st , 2012 – Infinia will complete fabrication and salt and sodium filling of Generation 3 Subscale Module
- Milestone #2 – May 30th, 2012 – Infinia will complete demonstration of the Generation 3 Subscale Module functionality
- Milestone #3 – August 31st, 2012 - Infinia will complete fabrication and salt and sodium filling of the Lab-Scale Module
- Milestone #4 – August 31st , 2012 – Infinia will complete Task #4, the System Design for 3kW with 12 hours storage
- Milestone #5 - November 30th, 2012 - Infinia will complete Task #2, demonstration of the Lab-Scale system functionality

Project Results and Discussion: Descriptive material for the six Phase I tasks identified in the Introduction of this report are detailed below and were condensed from over 100 pages of prior contract reports. What remains in this section is more of an overview that necessarily excludes much of the detailed test and evaluation, particularly with respect to the testing of three generations of subscale units where extensive testing with iterative hardware changes and test procedure changes were conducted to gain understanding of the fundamental processes involved in subscale unit operation. Most observed anomalies turned out to be artifacts of the subscale unit designs, but understanding the issues provided a much higher level of confidence for the lab-scale system design incorporating a 3 kW engine.

Note that the Task 1 discussion of the subscale module design also integrates Task 2 demonstration testing and results because the iterative subscale module design and testing that occurred during this process was so intimately integrated.

Task 1: TES Lab-Scale Module Design

Innovative Phase Change Thermal Energy Storage Solution for Baseload Power
Infinia Corporation

Given that the chosen PCM salt (NaF/NaCl eutectic) and the sodium heat transfer working fluid had never been tested together in the proposed system, the decision was made to first fabricate subscale devices in order to conduct some basic tests. These units provided valuable salt operational information and lessons learned. Design problems with the original subscale units resulted in two subsequent design iterations following the initial testing. The three generations of subscale test units are described first, followed by the lab-scale design that integrates with a 3 kW engine.

Subscale TES Evaluation Module Design

Generation1 (Gen 1) Subscale Module Design

In the first two of these devices (later called generation 1, or Gen 1) heat was extracted from the top of the device via a gas-gap calorimeter in lieu of a Stirling engine heater head. Multiple thermocouples embedded in the salt volume and vapor space allowed monitoring of salt and sodium temperatures. The high temperature hot plate used for conducting these subscale tests is shown with its plate component removed to show the electrical resistance heating element in Figure 2 (left). Figure 2 (right) is a schematic of the subscale module that illustrates where heat from the hot plate is applied at the bottom to melt the TES salt, which transfers heat to the lower density sodium pool boiler layer, vaporizing the Na and transporting the heat to the gas gap calorimeter by condensing on it. Two ¼" diameter tubes are connected to the gas gap calorimeter space. One is an inlet, the other an outlet for introducing a helium/argon mixture to the space to vary calorimeter effectiveness.

After extensive testing with the Gen 1 modules with inconsistent and inconclusive results, it was determined that a faulty execution of the Na fill procedure had over-pressurized the salt chamber and distorted the thin calorimeter diaphragm in one case and ruptured it in the other. This led to designing the Gen 2 modules described below with much thicker gas gap calorimeter diaphragms. Prior to that however, some important information about salt freezing characteristics was derived by subjecting the Gen 1 modules to x-ray analysis.

The x-ray images revealed that a salt "bridge" or "crust" spans the interior of the module about ¾ of the way up from the bottom of the vessel. The bridging behavior was previously observed during open-air tests. Furnace-heated crucibles of molten salt were allowed to cool in open air. When the first crystals begin to form at the surface of the molten salt, a thin layer across the top forms almost instantly, adhering to the walls of the container while the salt continues to solidify and shrink below the layer, forming a

Innovative Phase Change Thermal Energy Storage Solution for Baseload Power
Infinia Corporation

void. As seen in x-ray images, this also occurred within the subscale module when it cooled from the melt cycle performed earlier. Viewed in this light, much of the behavior of the subscale tests can be explained. This is discussed further below.

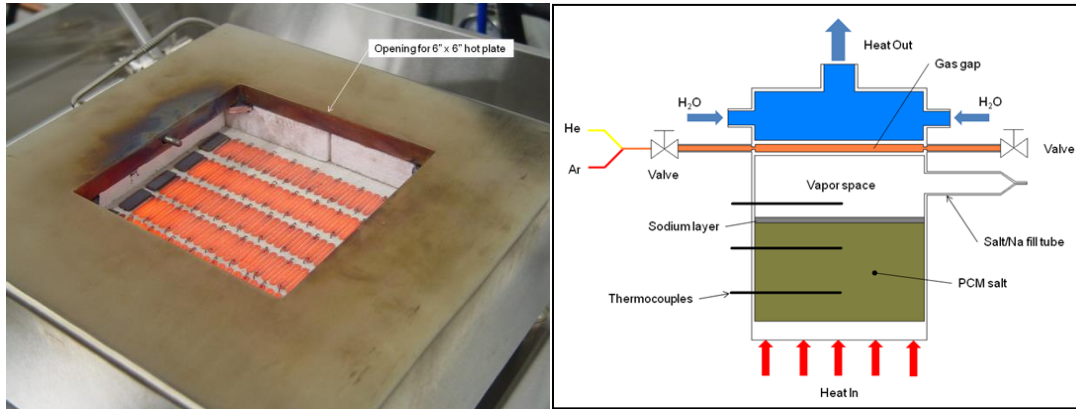


Figure 2, Hot Plate for Small-Scale TES Test Module (left) & Small-Scale TES Module Schematic, not to scale (right)

In subsequent testing, a tape heater wrapped around the vessel exterior prevented the salt bridge from forming so the liquid salt could contact the sodium pool. In one example a tape heater was wrapped about the salt vessel in the area of the maximum liquid salt level. The hot plate is turned off first, and the module is allowed to come to equilibrium. Then the tape heater is turned off. In this way, it was hoped that the formation of a salt bridge would be avoided. An x-ray of the module after cool-down confirmed the efficacy of this approach; the Na layer above the salt also was shown to greatly reduce the tendency to form the salt bridge.

Generation2 (Gen 2) Subscale Module Design

In response to the issues encountered in the two Gen 1 modules, two more Gen 2 subscale modules were designed and built, having the following primary differences and reasons behind the changes: 1) Gas gap calorimeter diaphragms thickened significantly to withstand sodium fill stresses; 2) Brazed construction replaced with welded joints to simplify construction and leak repair; 3) nickel base plate replaced with stainless steel to eliminate mismatch of coefficients of thermal expansion between it and the stainless steel used throughout the rest of the vessel; 4) Swagelok fittings for thermocouples eliminated in favor of a single thermo-well in the vapor space to eliminate potential leak paths.

Innovative Phase Change Thermal Energy Storage Solution for Baseload Power
Infinia Corporation

Test results for this module were encouraging, and confirmed basic operation. During heat-up, the calorimeter cooling function was disabled. This was because earlier testing revealed that conduction losses through the vessel wall permitted a thermal “short circuit” around the calorimeter, making it difficult to heat the salt effectively. The vessel wall is relatively thick adjacent to the calorimeter plates. When liquid coolant is flowing through the coolant space, the wall temperature is relatively low; on the order of 40°C. Wall temperature at the lower calorimeter plate is high; 700°C or more. This sets up a large temperature gradient, and thus high heat transfer across the thick wall section. To combat this problem during heat-up (charging), it was also decided to use air to cool the calorimeter space during the cool-down only. The use of air avoids boiling of liquid coolant (propylene glycol) when the module is hot.

The temperature plots shown in Figure 3 (left) show the temperatures within the salt as well as the vapor space from about 500-550°C through about 720°C. As the salt temperature exceeds about 550°C, the sodium pool boiler begins to function more effectively, and the vapor space temperature tracks the uppermost salt temperature very closely. The salt phase change is seen to occur at the expected temperature of about 680°C, for approximately 20 minutes. The lower thermocouple T/C 1 is located nearest the heat source, and is seen to indicate rapid superheating of the salt in this area. Finally, it can be seen that the salt temperature in the center of the vessel (T/C 2) shows the salt in this area is the last to fully melt. This suggests that liquid salt being heated from below makes its way to the top of the salt mass, presumably due to the reduction in density, and heats the upper salt region somewhat before the middle. This is in line with expectations.

With the salt fully melted and temperatures within it reach a steady-state condition, air is flowed through the coolant space, and the heat source is turned off. The resulting temperature plot is shown in Figure 3 (right). Vapor space temperature as well as the lower calorimeter plate track the salt mass temperature very well, with a small temperature drop throughout most of the salt phase change. At around 190 minutes, the sodium vapor temperature lags that of the salt to a significantly greater degree. This is likely due to salt crust formation at the salt/sodium interface. The salt has poor thermal conductivity, and thus impedes heat transfer to the sodium pool. Approximately 75-80% of the salt’s latent heat is extracted before the vapor space temperature starts to drop. Also of note is that the central region of the salt stays hot the longest; heat is being extracted at the upper surface by the pool boiler, while the bottom of the vessel loses heat by convection since it is not insulated.

Innovative Phase Change Thermal Energy Storage Solution for Baseload Power Infinia Corporation

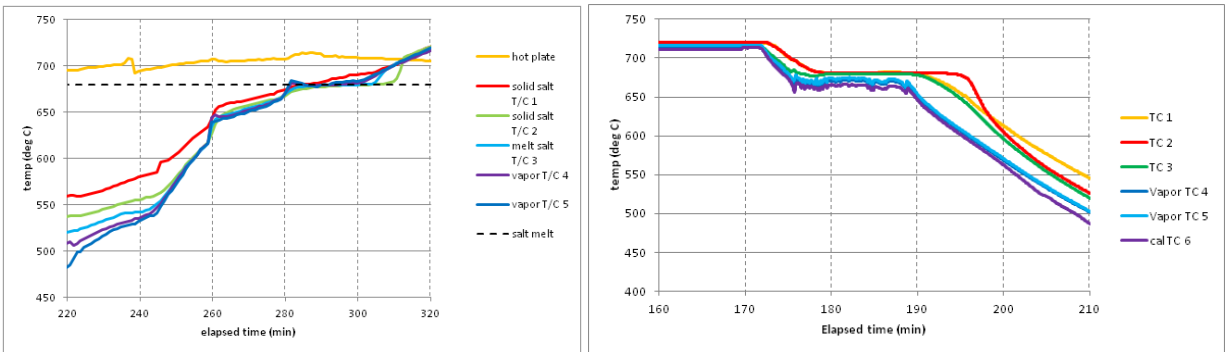


Figure 3, Second Gen 2 Module Charge Data (left) and Discharge Data (right)

Generation3 (Gen 3) Subscale Module Design

As mentioned earlier, there are design flaws inherent in the Gen 2 module design that preclude a full investigation of proper functionality of the Baseload concept. These include the following: 1) Thermal short circuit around the calorimeter; 2) input heat flux not representative of anticipated solar levels; 3) excessive insulation losses.

In addition, Infinia desired to investigate the effect of tapering the vessel side walls in order to provide a means for liquid salt to displace the solid salt mass and escape to the surface during heating.

A third iteration of subscale hardware, known as Gen 3 was designed to address the above-mentioned items of interest. The overall objective of the Gen 3 hardware was to fully validate the functional aspects of the Baseload concept, and to then apply the lessons learned to larger scale hardware; specifically the lab-scale one-hour demonstrator. Specific objectives included the following:

1. Demonstrate key functional characteristics
 - a. Melt phase-change salt in a similar manner to plan for lab-scale configuration
 - b. Have liquid salt migrate to the top and vaporize sodium as the salt melts
 - c. Maintain the liquid salt/sodium interface until virtually all the salt is solidified during discharge
 - i. Requires prevention of salt crust formation
 - ii. Requires locally frozen salt crystals at the sodium interface to sink
2. Validate design elements
 - a. Demonstrate that the taper works to provide a liquid salt path
 - b. Input flux same as solar: $\sim 30 \text{ W/cm}^2$

Innovative Phase Change Thermal Energy Storage Solution for Baseload Power
Infinia Corporation

3. Improve instrumentation and data collection to enable more rigorous conclusions
 - a. More salt mass temperature data
 - i. Salt melt/freeze dynamics
 - b. Heat rejection calorimetry
 - i. Characterization of latent heat extraction efficiency
 - c. Experimentally characterize insulation losses
 - i. Enables accurate energy balance calculations

A cross-section of the Gen 3 module is shown in Figure 4. The module is fabricated entirely from stainless steel 316L, and is of welded construction. Residing in the Na vapor space is a tubular, helical coil calorimeter through which nitrogen flows, serving to simulate the Stirling generator. Two thermo-wells protrude a short distance into the vapor space to measure the sodium vapor temperature, while three more thermo-wells extend vertically into the salt mass to measure its temperature at various radial and axial locations. The salt mass for this device is 4.7 kg, which represents approximately 900 W-h of latent heat energy. The sodium inventory is 290 grams.

In order to provide higher heating rates Gen 3 switched to susceptor-based heating. A susceptor uses an inductor coil to heat an intermediate object to a very high temperature, which in turn heats the target by radiation from that intermediary.

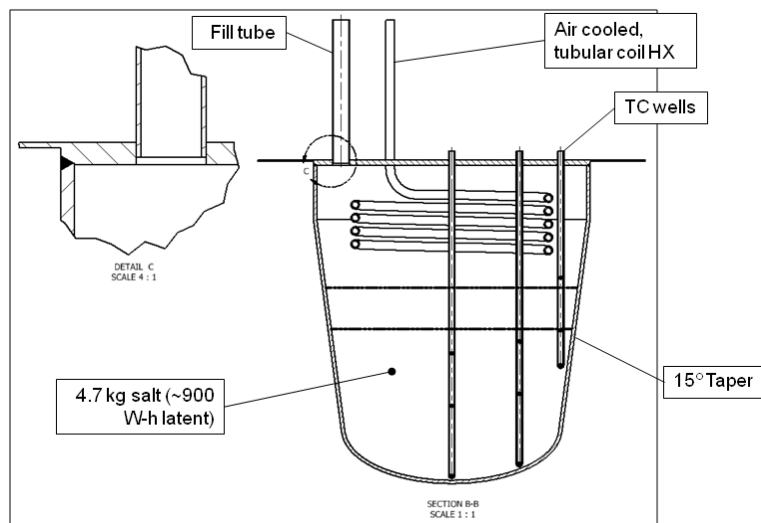


Figure 4, Gen 3 Subscale Module

This arrangement was successfully employed to heat the Gen 3 modules. A stack of rigid high temperature insulation boards were machined such that a cavity is formed,

Innovative Phase Change Thermal Energy Storage Solution for Baseload Power
Infinia Corporation

into which the module is placed. A diagram of the susceptor heating the Gen 3 device is shown in Figure 5. The induction coil and SiC rings are located at the bottom. In this configuration, the bottom of the TES vessel is heated, with the tapered side-wall receiving some heat as well. Side-wall heating has proven important to prevent salt bridging – the formation of a salt crust at the sodium/salt interface, particularly when melting the eutectic salt for the first time.

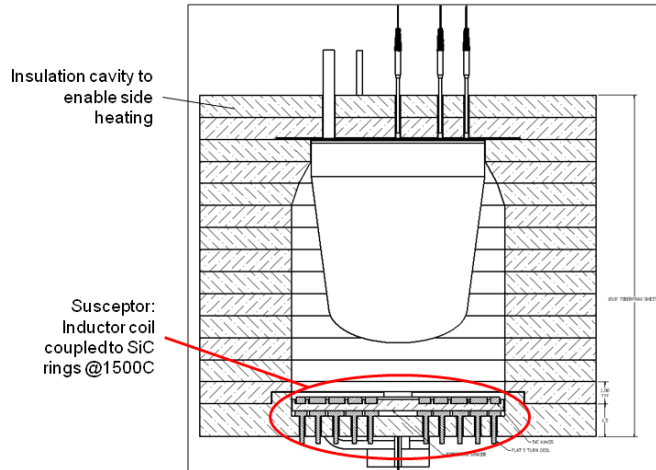


Figure 5, Gen 3 Module Susceptor Heating

Four separate tests for this hardware were conducted to evaluate subscale objectives:

1. Characterization of insulation losses: The goal is to use calorimetry to generate a data set plotting insulation losses versus temperature, needed for energy balance calculations.
2. Sodium pool boiler function: The goal is to both verify pool boiler functionality and generate a data set plotting inductor power supply duty cycle settings versus net input power. The latter goal is necessary in order to quantify the induction heater characteristics.
3. Fast heating: The goal is to characterize the ability of the device to accept heat at the specified desired flux level when the “engine” is both off and on (HX rejecting heat or not).
4. Slow heating: The goal is to characterize the temperature differentials within the salt during steady state and discharge modes, as well as the efficiency of energy extraction.

Innovative Phase Change Thermal Energy Storage Solution for Baseload Power
Infinia Corporation

A total of three Gen 3 modules were fabricated. The first module, charged with sodium only, was used to conduct the pool-boiler- only test (Tests #1 and 2 above), while the second module, charged with salt and sodium, was used to conduct Tests #3 and 4. The third module serves as a spare.

The first test completed was a characterization of insulation losses.

The next test involved operating the Gen 3 module as a pool-boiler only. In this test, heat was extracted from the module by flowing nitrogen through the internal heat exchanger. The extracted heat is calculated in real time by calorimetry using the flow rate of the nitrogen, average specific heat and the differential of the inlet and outlet temperatures. The Gen 3 modules performed very well in pool-boiler-only mode as expected. The difficulty with the heat rejection system encountered in earlier generation designs was eliminated, although at the expense of a limited maximum operating range.

In preparation for conducting Tests 3 and 4, another Gen 3 subscale module was charged with NaF-NaCl eutectic salt and sodium. After the full charge of 4.7 kg of the salt was put into the vessel, melted and fused, the sodium was introduced. The mass of sodium used for the pool boiler is based on reverse-engineering the data reported by Adinberg in the original NaCl-based demonstration [Adinberg et al, 1999]. Given the reported size of the vessel, the mass of both the NaCl and sodium used, and the solubility of sodium in the salt, a sodium pool depth of approximately 10 mm was calculated. Assuming a similar solubility of the sodium in the NaF/NaCl eutectic yields a required mass of 290 g.

Tests 3 and 4 were conducted and generally validated the objectives defined above. The rapid heating was done as fast as possible within the constraints of the upper temperature limits of the vessel exterior ($\sim 850^{\circ}\text{C}$) while the internal calorimeter heat exchanger (HX) was disabled (nitrogen coolant flow rate set to zero), then, the heat was turned off and the HX set to a constant rate. The full data set is shown on the left in Figure 6 (left), which included three successive runs with HX reject rates for 60, 75 and 45 lpm nitrogen flow respectively. At approximately 116 minutes, the heater is turned off, and the flow of nitrogen through the HX is turned on. Reject heat spikes to around 810 W, then decreases as energy is extracted from the superheated salt. At about 132 minutes, the salt begins to freeze, and latent heat energy is extracted from the salt at an average rate of about 725 W for 25-26 minutes. This time span is labeled "HX" on the right in Figure 6. This clearly illustrates how the relevant thermocouples track within a few degrees for about 2/3 of the latent heat energy extraction period. At

Innovative Phase Change Thermal Energy Storage Solution for Baseload Power Infinia Corporation

that point, the top of the liquid salt layer crusts over and traps the Na above that point while about 1/3 of the salt is still molten beneath it. Thermocouples T2 and T5 near the center of the salt volume remain at the melt point for about another 12 minutes showing that that portion is still partially liquid. The slow heating test 4 results confirmed the same basic information.

The theoretical latent energy content for 4.7 kg of NaF-NaCl salt is 898 W-h. Thus, from a total latent energy content of the salt, about 33% was extracted at the HX, 31% was lost to the environment, and the remaining 36% was not accessible after the salt solidified at the sodium pool/salt interface. This result was generally consistent for all three HX flow rates tested, whereby a third of the salt's latent energy was consumed at the HX, a third lost through the insulation, and a third "trapped" after the outer layer solidifies.

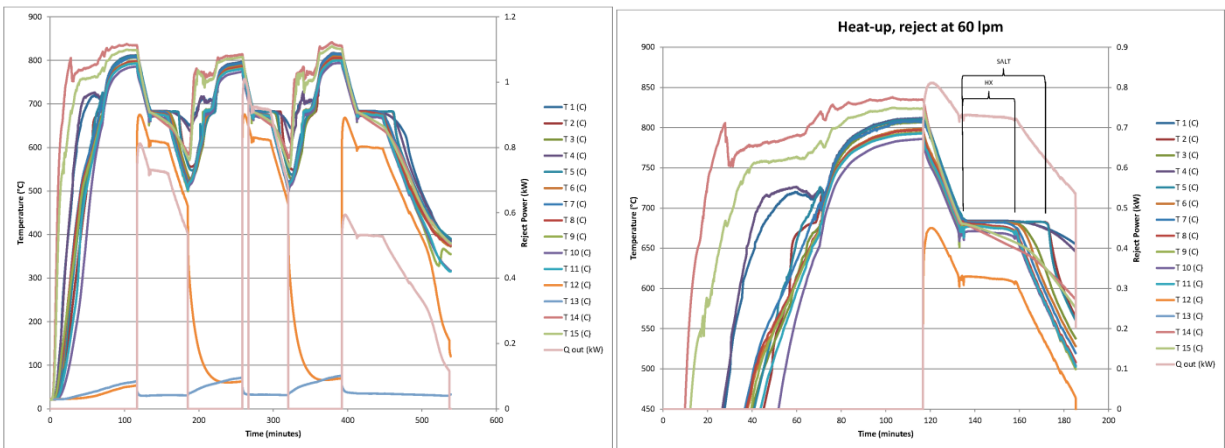


Figure 6, Test 3(a) Full Results (left) and 60 lpm HX Detail (right)

Gen 3 Subscale Conclusions

A set of criteria were established during the development of the Test Plan to determine if our objectives have been met. The test results will be discussed with respect to the above objectives in the following.

1. *Module must meet the target input flux levels:* The target average flux level is 35 W/cm². This is a conservative value based on the design heat flux of Infinia dish-engine heater heads. However, testing showed that levels estimated to be on the order of only 15 W/cm² are attainable without exceeding allowable vessel temperatures. This lower flux can be achieved by the proper development of the flux profile in the optical design phase.

Innovative Phase Change Thermal Energy Storage Solution for Baseload Power
Infinia Corporation

2. *Sodium vapor temperature reaches the salt temperature quickly:* In reality, tests show that the vapor space temperatures lag salt temperatures until the entire salt mass is molten. This means that upon initial start-up, the internal HX does not extract meaningful energy until the salt temperature is quite high. In a larger-scale device coupled to a Stirling generator, provisions should be made to transfer heat to the sodium pool faster, such that the engine can start producing power as soon as practicable.
3. *Sodium pool boiler can transfer required energy:* Testing demonstrates that the pool boiler is effective at transferring energy to the internal HX at sodium temperatures above about 550°C, and is very responsive to changes in power input and extraction.
4. *Sodium pool boiler in the presence of salt can transfer required energy:* Test 2 (pool boiler only) data show that the Gen 3 module reaches a steady-state condition whereby the vessel temperature is ~680°C when the susceptor duty cycle is 10% and the HX nitrogen flow rate is 60 liters per minute. The HX reject rate, as calculated with nitrogen gas calorimetry is 757 W at these conditions. In reviewing the data of Test 3(a) 7 May 2012, when the HX flow rate is 60 lpm and the device is extracting energy in the salt latent phase, the vessel temperature is similarly about 680°C, and the measured heat reject rate averages about 725 W. Thus, it appears that the salt itself has a minimal impact on the pool boiler functionality.
5. *Sodium vapor space closely tracks molten salt temperature:* Tests 3 and 4 both confirm that the vapor space temperature is close to the molten salt temperature. The caveat here is that this is true so long as a layer of solid salt has not formed at the sodium pool/salt interface. The data suggests that liquid salt can become trapped below a solid crust, and features to help avoid this phenomenon should be considered.
6. *Isothermal salt mass indicates molten salt convection:* As would be expected, there exists a significant thermal gradient in the salt when heating. This gradient is primarily seen in the axial sense, and is far more pronounced when the salt is solid as opposed to its liquid state. This suggests that there could be some convection cells within the liquid salt, causing the temperature to become more uniform.
7. *Meet target internal HX rejection levels:* The Gen 3 module was able to achieve the expected rates of heat extraction for the chosen HX coil geometry and nitrogen flow rates.

Innovative Phase Change Thermal Energy Storage Solution for Baseload Power
Infinia Corporation

8. *Sodium vapor temperature closely tracks salt temperature throughout the solidification phase:* As reported in the testing results, the vapor temperature is close to the salt temperature, although it does drop perceptively while the salt stays constant. In addition, the vapor temperature only tracks the entire salt volume's temperature for about two-thirds of the solidification time duration.
9. *Energy rejected during discharge is 90% of theoretical salt latent energy:* The rejected energy amounts to about 33% of theoretical. Another 30-40% is lost to the environment, and some fraction of this could potentially be recovered with better insulation. The balance of latent energy is not available to the pool boiler due to a significant portion of the liquid salt being trapped beneath a crust of salt which probably forms at the sodium pool/salt interface as discussed before. Again, design features to avoid this problem must be considered in future devices.

Lab-scale TES Module Design

At the conclusion of the battery of tests conducted with the Gen 3 subscale module, a workshop was conducted to review the results and define the attributes of a lab-scale device. The lab-scale device will be coupled with an Infinia Stirling generator, and will be designed to generate 3 kW-h of electrical energy. The following design requirements were developed for the lab-scale demonstration unit:

- Salt mass sized for thermal-to-electrical efficiency of 25%;
- Salt mass sized for latent heat energy 3x theoretical based on subscale results;
- Sodium mass based on 4% molar solubility and 10mm pool depth;
- Maximum heat flux shall be 15-17 W/m² based on subscale results;
- Salt vessel shape shall permit liquid salt escape path to the sodium pool;
- Salt vessel shall be constructed of stainless steel;
- Lab-scale heater shall be radiant-based;
- Thermocouple instrumentation shall be limited to the vessel exterior;
- Thermosiphons will be added to the vessel interior, in contact with the salt volume.

The primary design difference between the sub and lab-scale modules is the introduction of the thermosiphons. The purpose of the thermosiphons is two-fold. The first is to address the issue of the formation of solid salt at the sodium pool interface during heat extraction, which traps and isolates liquid salt from the pool boiler, inhibiting heat transfer. Several thermosiphons embedded in the salt volume, extending vertically

Innovative Phase Change Thermal Energy Storage Solution for Baseload Power
Infinia Corporation

from above the sodium pool, down to the vessel bottom, should permit further heat transfer from the liquid in the central area of the vessel; even after the top surface has solidified. The second reason for adding the thermosiphons is to allow some heat transfer from the vessel bottom, directly to the sodium pool during the charging phase. Conceptually, it was envisioned that liquid salt would rise to the sodium pool during heat-up in the space between the vessel wall and the solid salt due to the liquid salt's lower density. Subscale testing suggests that does not occur in a significant way as evidenced by the vapor space temperature lag with respect to the salt temperature. The thermosiphons will provide a direct energy path from the area where the vessel is heated, to the sodium pool, such that the Stirling engine can begin to function shortly after heating starts.

The salt mass is found to be 180 kg based on the above assumptions for thermal-electric conversion efficiency, the ability of the subscale module to extract latent heat from the salt, and the reported heat of fusion of the NaF-NaCl eutectic of 0.191 kW-h/kg.

The shape chosen for the salt bath section of the vessel is spherical. This shape has several advantages, such as maximizing volume per unit of surface area, ensuring a liquid salt escape path (salt cannot get trapped between the heated shell structure and the solid salt due to geometry), and it is a readily available shell from ASME tank suppliers.

The upper section of the storage vessel is conical. This shape was chosen to "funnel", or direct sodium vapor to the Stirling generator heater head. In addition, the cone shape is also a readily available shell from ASME tank suppliers.

The Stirling generator is oriented vertically, with the engine heater head hermetically welded to the top of the vessel cone. A 1.25" diameter tube in the cone section is used for filling the vessel with salt. This tube will be sealed by welding a cap over the tube once the salt fill is accomplished. A second 0.5" tube fitted with a bellows valve is used to inject sodium into the vessel. A total of four 0.5" diameter thermosiphons are located in the hemispherical section of the vessel: one at the axial centerline, and three others placed radially at about $\frac{1}{2}$ the vessel diameter, spaced 120° apart. A thick flange from which the entire module will be suspended is welded to the vessel's conical skirt.

Innovative Phase Change Thermal Energy Storage Solution for Baseload Power
Infinia Corporation

Heating of the vessel will be done with a radiant-based heater supplied by Sandvik Wire and Heating Technology, whereby the diameter of the heating target is that of the TES vessel hemisphere, and the heating rate required was found to be 30 kW. This will result in an average flux for the maximum 30 kW power level over the hemisphere's projected area of 6.8 W/cm^2 . This is less than half of the current maximum flux level found by experimentation that causes vessel overheating.

The lab-scale module is suspended over the heater by the vessel flange. A total of six rods used to hang the device are isolated from a stationary framework by die springs. These springs dampen the force transmitted by the generator vibration to the framework. A section showing the test stand layout of the lab-scale module along with the heater is shown in Figure 7.

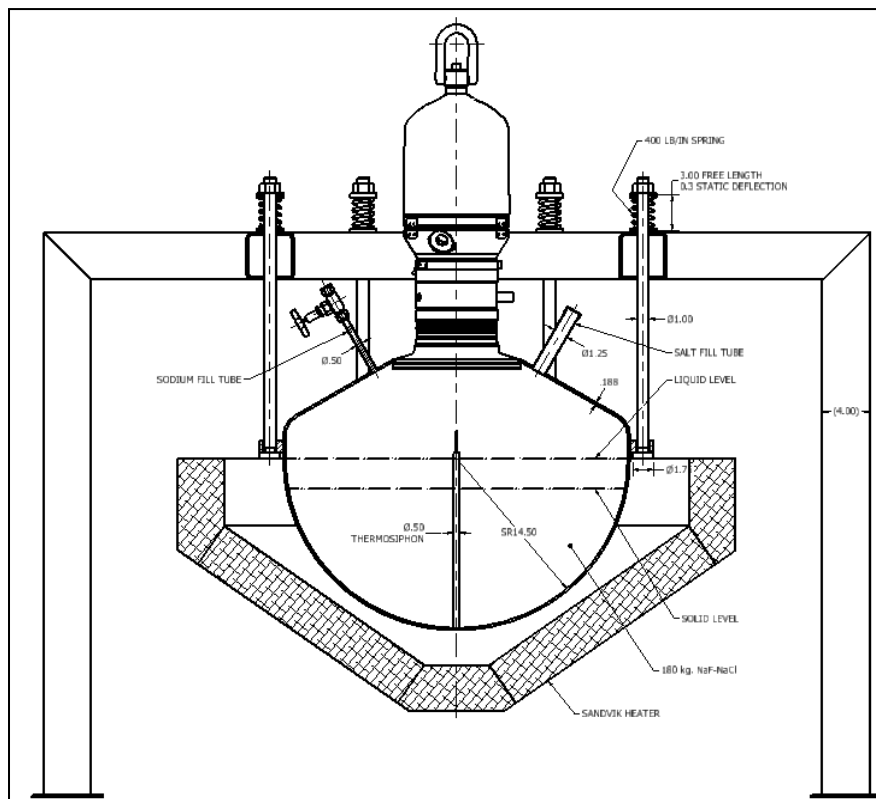


Figure 7, Lab-Scale Test Stand Layout

Task 2: TES Module Lab Demonstration

Figure 8 shows the locations of the 26 thermocouples attached to the module and test stand. These identifiers are referred to in the discussions that follow. Locations 1

Innovative Phase Change Thermal Energy Storage Solution for Baseload Power
Infinia Corporation

through 6 are located axially along the vessel exterior as shown, while location 7 is on the back of the generator heater head. The alpha designators A, B and C refer to the radial positions spaced approximately 120° apart. Location 8 refers to two shallow thermocouple wells protruding into the sodium vapor space, about 180° apart. Locations 9 and 10 are used to monitor the temperature of the vessel support rods, while the thermocouple at location 11 tracks the temperature of the bellows valve. Generally, the temperatures at any given axial (numeric) location are similar enough that for the purposes of clarity only one radial position is used for reporting.

Temperature set-points were gradually increased to a maximum of 750°C over the span of about 3-1/2 hours. The generator self-started very early during the heating, and was kept to a low power output by commanding minimum stroke voltage; about 10 watts.

When the vessel temperature reached about 725°C, the stroke voltage was increased. The generator maintained an output of 120-150 W while heating continued.

After over 4 hours' time, the stroke voltage was again increased, but the generator output could not be maintained and power fell immediately in a linear fashion. Stroke was increased two more times with similar results; indeed the heater head temperature fell almost 150°C and did not recover. Figure 9 shows a plot of vessel temperatures and generator power during this test.

Figure 10 below shows this event in detail. It was determined that there was not sufficient heat transport to the heater head to support continuous operation of the generator anywhere near the nominal design point of 3 kW, and that the heater head was being heated strictly by conduction and radiation alone; no two-phase heat transfer from the pool boiler occurred. Thus, it was evident that there was not sufficient sodium present in the device, and plans were made to add more. After a day's cooling, the module was removed from the test stand and re-connected to the sodium filling station.

On 5 December 2012, another sodium fill attempt was made. Another charge from the fill vessel brought the total sodium in the module to 7.7 kg; a full 1.2 kg beyond our original target of 6.5 kg. The module was again disconnected from the sodium fill apparatus and installed in the test stand for further testing.

Innovative Phase Change Thermal Energy Storage Solution for Baseload Power
Infinia Corporation

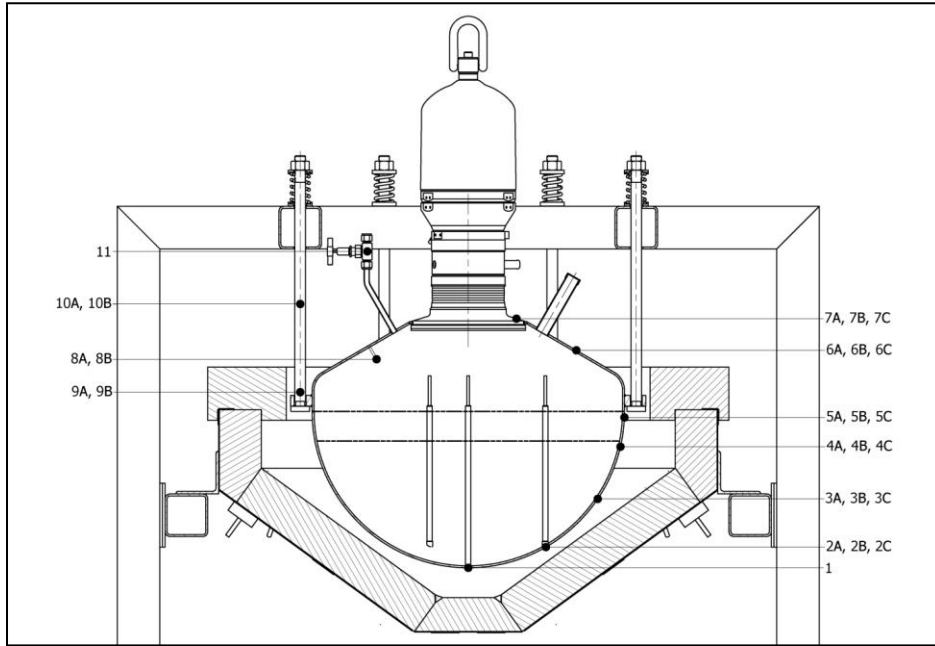


Figure 8, Thermocouple Locations

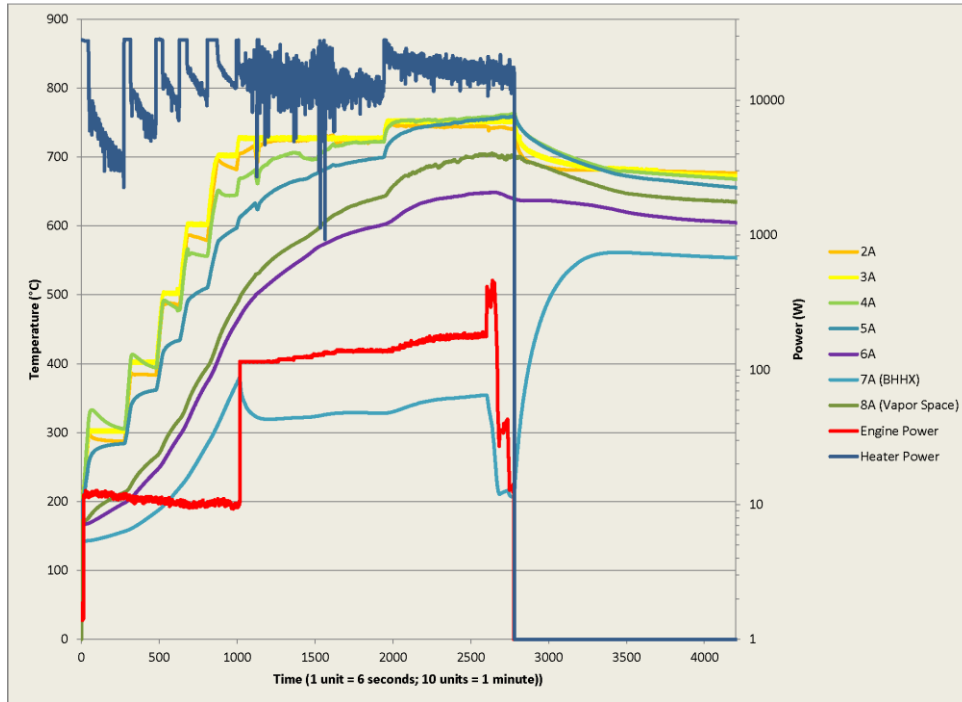


Figure 9, December 3 2012 Full Test

Innovative Phase Change Thermal Energy Storage Solution for Baseload Power
Infinia Corporation



Figure 10, December 3 2012 Generator Run Detail

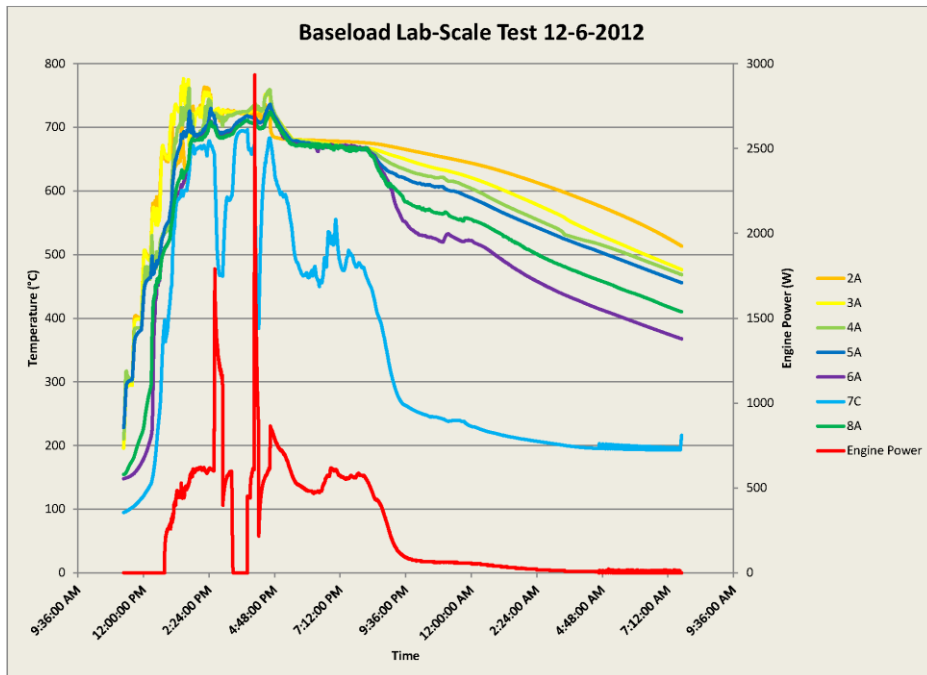


Figure 11, December 6 2012 Full Test

Innovative Phase Change Thermal Energy Storage Solution for Baseload Power
Infinia Corporation

Figure 11 above shows vessel temperatures and generator power during this test. As before, the temperature set-point was increased gradually, this time to a maximum of 780°C. Generator output was varied by changing stroke voltages to determine the effect on system temperatures. Peak heater head temperatures were much higher during this test indicating that the pool boiler is functioning. However, the heater head temperature and power output both drop rapidly with increased demand, which shows that heat transport via the pool boiler is still limited. At 4:38 pm, the radiant heater is turned off and the generator is allowed to run at maximum stroke voltage while the salt cools. A detail of this is shown in Figure 12. As can be seen in the plot, the total electrical energy generated during discharge is about 2.7 kW-h; very close to the goal of 3 kW-h.

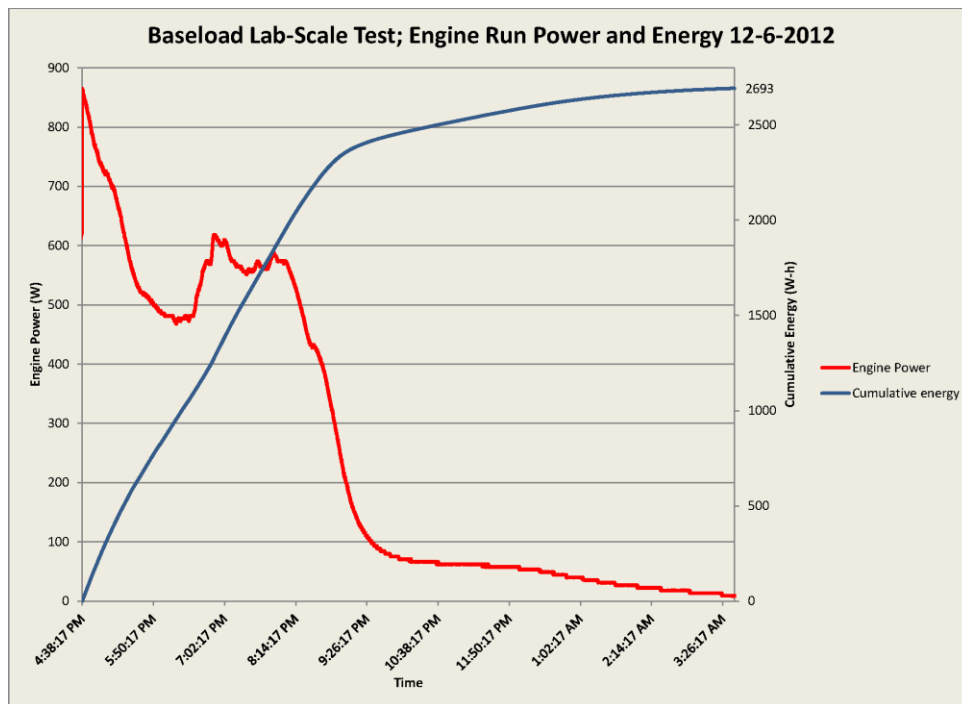


Figure 12, December 6 2012 Generator Run Detail

At this time, the Infinia team was scheduled to travel to DOE HQ in Washington, DC to attend the formal continuation review. Although the test run of 6 December supported the idea that the device may still be limited by too little sodium, there was not time to add more prior to the meeting. It was therefore decided to conduct one more test run the following day. The purpose of this run would be to find the optimum generator output level. In other words, keep the temperature set-point at a given value, and find the stroke voltage that maintains generator output at equilibrium. Then, turn off the heater

Innovative Phase Change Thermal Energy Storage Solution for Baseload Power
Infinia Corporation

and let the module run at that stroke voltage. The results of this test are discussed below.

Figure 13 below shows vessel temperatures and generator power during this test. The temperature set-point was raised to a maximum of 750°C (note that the starting temperature is about 400°C from the previous day's test), and the stroke voltage values adjusted until output power achieves equilibrium.

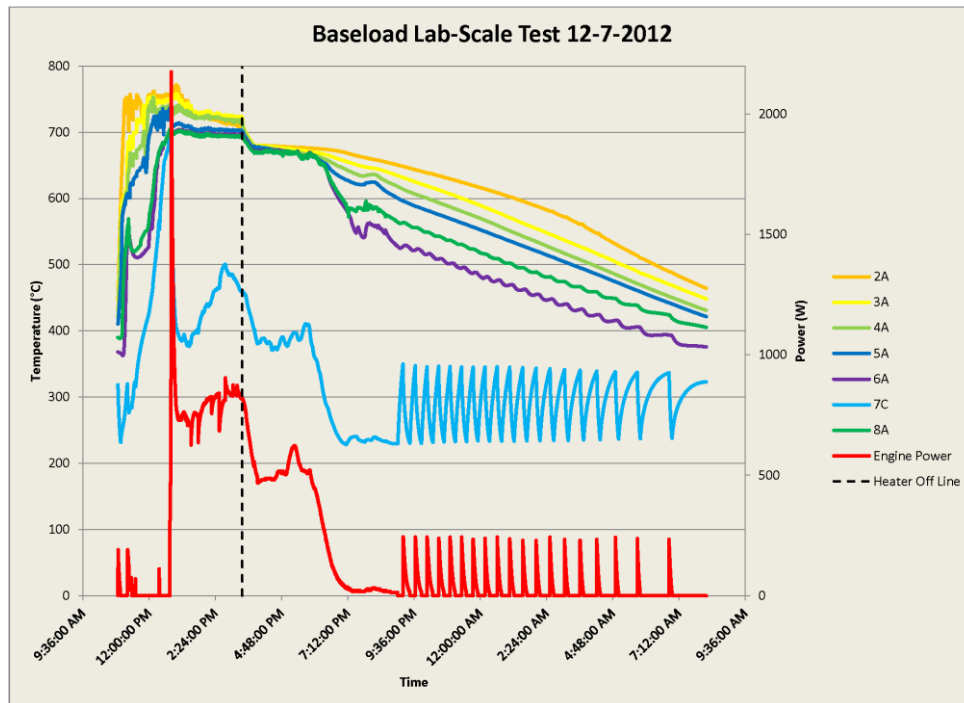


Figure 13, December 7 2012 Full Test

At about 12:48 pm, the heater is turned off, and the module is allowed to discharge.

The plot in Figure 14 shows the changing of stroke commands until generator output equilibrium is achieved, while Figure 15 shows detail of the discharge and cumulative electric energy generated.

Although the general shape and extrema of the power output curve of Figure 15 is quite similar to that of the previous day's run, the generator energy production of about 1.8 kW-h is markedly reduced. The conclusion drawn is that it is generally advantageous to command maximum generator stroke upon TES discharge.

Innovative Phase Change Thermal Energy Storage Solution for Baseload Power
Infinia Corporation

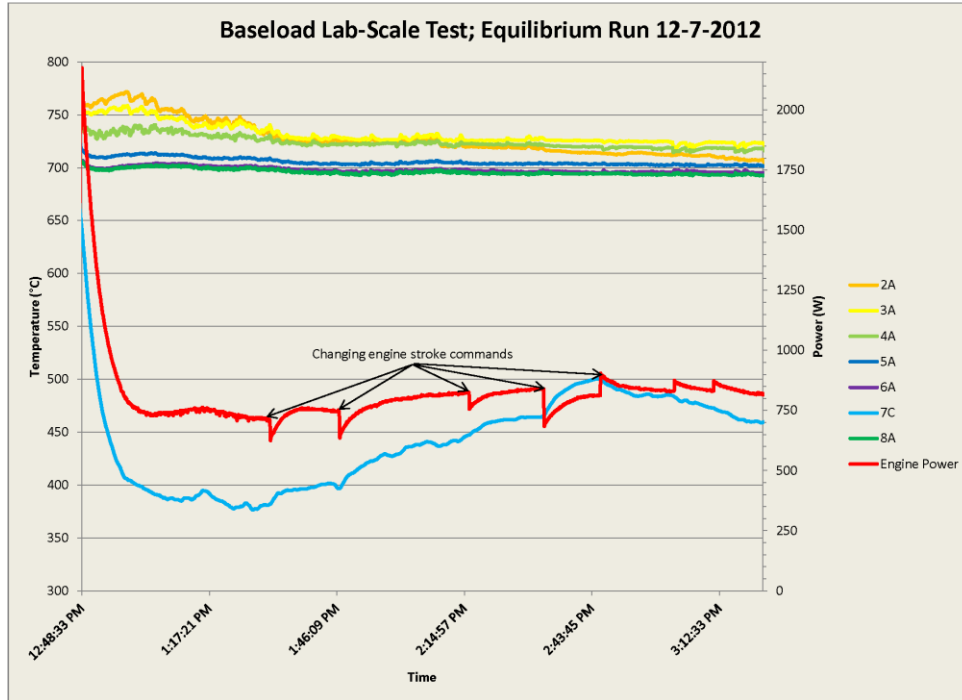


Figure 14 December 7 2012 Optimizing the Generator Stroke Voltage

Test results to this point were discussed in Infinia's presentation to DOE personnel during the Phase 1 Continuation Review of 11 December 2012. It was decided during that meeting to add another charge of sodium and conduct further testing and evaluation.

On 14 December 2012, the module was again removed from the test stand and connected to the sodium fill rig. Two charges from the fill vessel were added to the module for a total of 11.3 kg sodium. The module was again re-installed into the test stand.

Figure 16 below shows the vessel temperatures and generator power during this test. The module was heated step-wise as before. After the generator self-started, the stroke voltage was held at a minimum to facilitate heating of the salt. After all of the vessel temperatures reached approximately 750°C, the stroke voltage was increased until the engine was producing about 2.9 kW. At this point, the system was allowed to run in a steady state condition in order to assess the ability of the pool boiler to maintain the generator output at nominal levels. This test was successful; all temperatures including the heater head stabilized over the 2+ hours' duration of this part of the testing.

Innovative Phase Change Thermal Energy Storage Solution for Baseload Power
Infinia Corporation

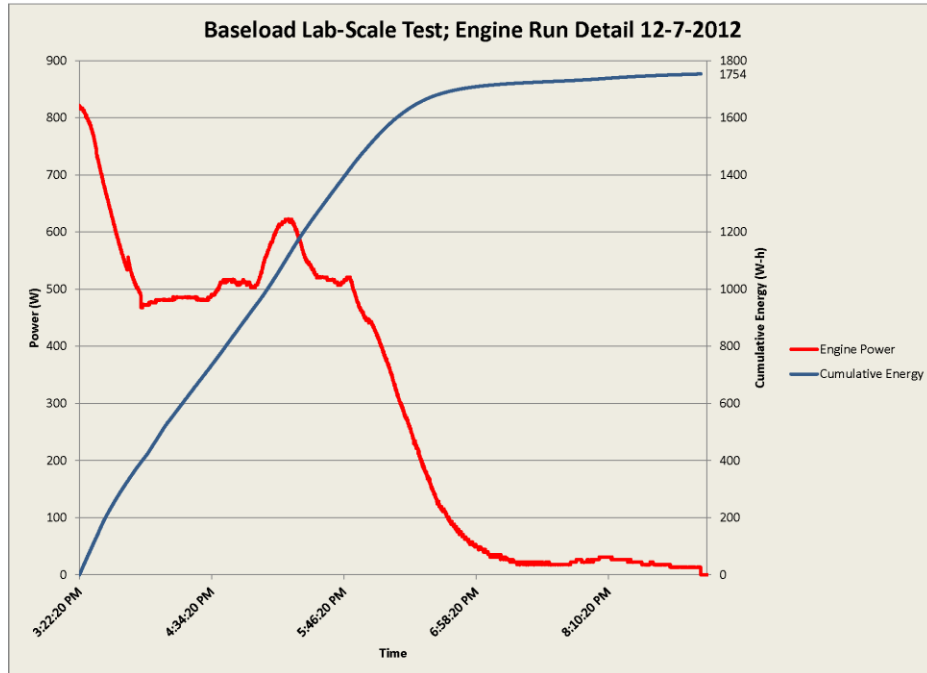


Figure 15, December 7 2012 Generator Run Detail

At about 2:54 pm, the power to the radiant heater was shut off, and the system was allowed to discharge at its maximum rate (maximum commanded stroke voltage). Figure 17 below shows the generator run detail and cumulative electrical energy produced.

The generator power stays fairly constant at about 3 kW during the salt liquid superheat region, and declines steadily throughout the solidification phase. Total energy produced is just over 3.2 kW-h, which satisfies the Phase 1 goal.

During evaluation of the data gathered during this test, it was noticed that although the system appeared to be in a steady state condition, the heater power was inexplicably high. This can be seen in the plot of Figure 18. Heater power was found to be about 15 kW and dropping at the conclusion of the steady state run. At full operating temperature, the engine efficiency is assumed to be about 30%. This would mean that the thermal energy consumed is 10 kW while the generator is producing 3 kW electrical power. Another 2.5 to 3 kW insulation losses were calculated, which implies that the additional heater power level is being absorbed, presumably by the salt. In other words, the team suspected that salt melting was incomplete.

Innovative Phase Change Thermal Energy Storage Solution for Baseload Power
Infinia Corporation

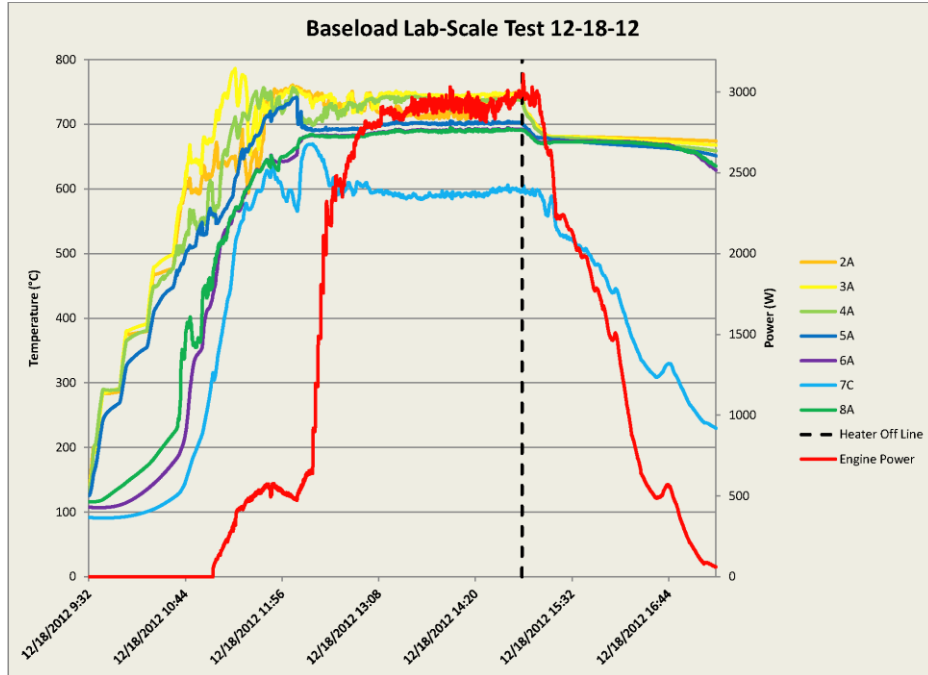


Figure 16, December 18 2012 Full Test

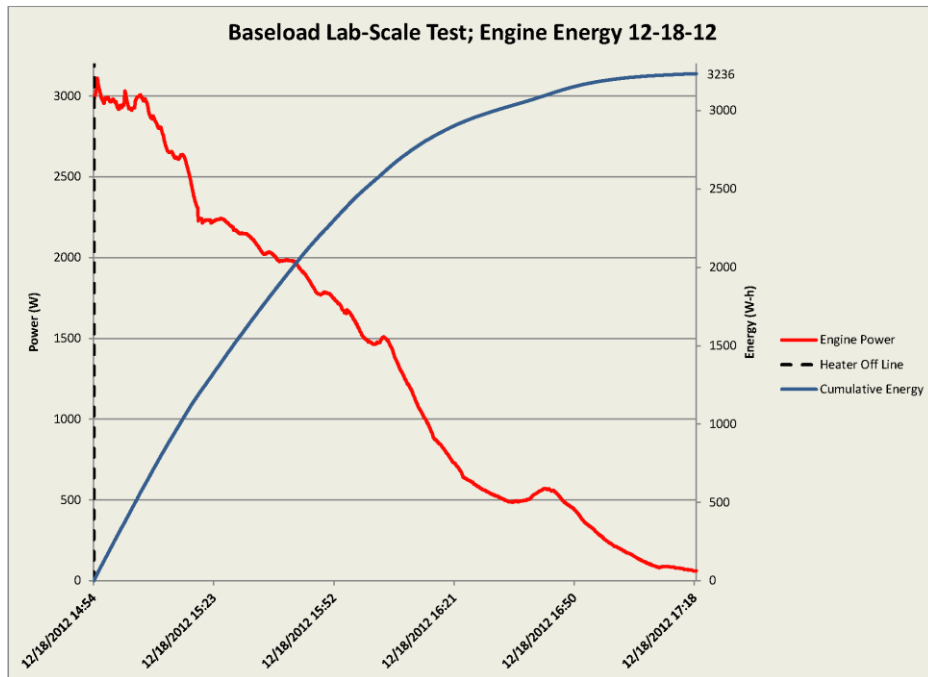


Figure 17, December 18 2012 Generator Run Detail

Innovative Phase Change Thermal Energy Storage Solution for Baseload Power
Infinia Corporation

It was therefore decided to attempt yet another test run to see if the heater power would reach an equilibrium level. This test was run the following day.

Figure 19 below shows the vessel temperatures and generator power during this test. Heat-up occurred from a higher temperature, since the module was still fairly hot from the day before. A key difference from the previous day's test was that the commanded stroke voltage stayed at a minimum throughout the salt melt and steady state period. This kept the generator thermal consumption low for a quicker test. Heater power was watched carefully for equilibrium conditions. As shown in Figure 20, the heater power gradually diminished until leveling out at about 6 kW. Also shown in the figure are the rejected heat as found from calorimetry of the cold heat exchanger, and the insulation losses as calculated from an energy balance of the heater power, generator power, and reject heat. This figure is about 3.5 kW at 750°C; about 20% higher than expected.

After the heater dropped to a constant level indicating equilibrium had been accomplished, it was assumed that the entirety of the salt mass had been melted in contrast to earlier efforts. At this point, the heater is turned off, the generator stroke voltage increased to maximum, and the system is permitted to discharge at its maximum power as before (Figure 21).

Not surprisingly, the generator was able to produce a bit more energy from the additional molten salt mass. The total energy was almost 3.9 kW-h as compared to 3.2 kW-h from the day before. It should be noted that based on the mass of salt in the system, the expected energy produced is up to 6 kW-h.

At this point, the project period of performance had ended, and further testing was deemed unnecessary unless further hardware modifications could be attempted as part of a Phase 2 continuation award.

Unfortunately, the DOE contract monitors decided not to pursue further funding for this project; however a no-cost extension was granted for Temple University to complete their research study on the physics of solid/molten salt dynamics. Their report is submitted to DOE under separate cover.

Innovative Phase Change Thermal Energy Storage Solution for Baseload Power
Infinia Corporation

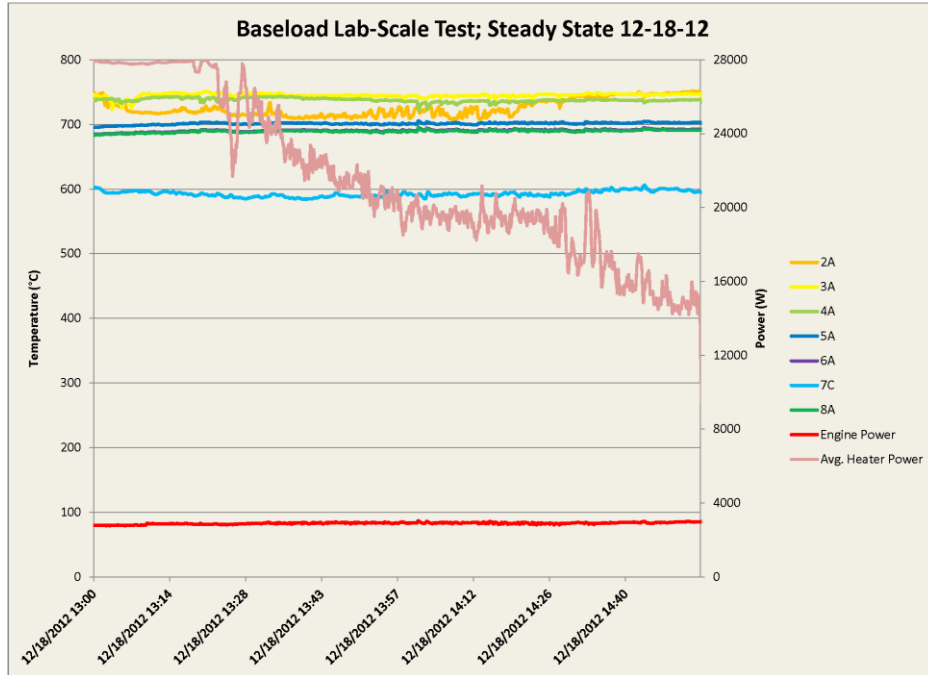


Figure 18, December 18 2012 Steady State Showing Heater Power

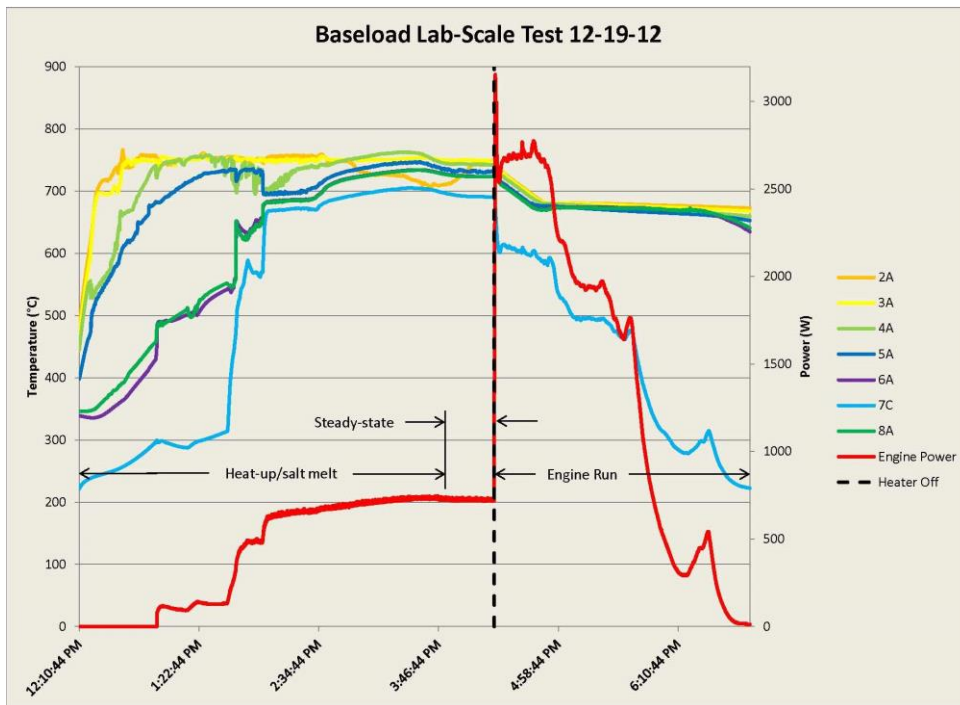


Figure 19, December 19 2012 Full Test

Innovative Phase Change Thermal Energy Storage Solution for Baseload Power
Infinia Corporation

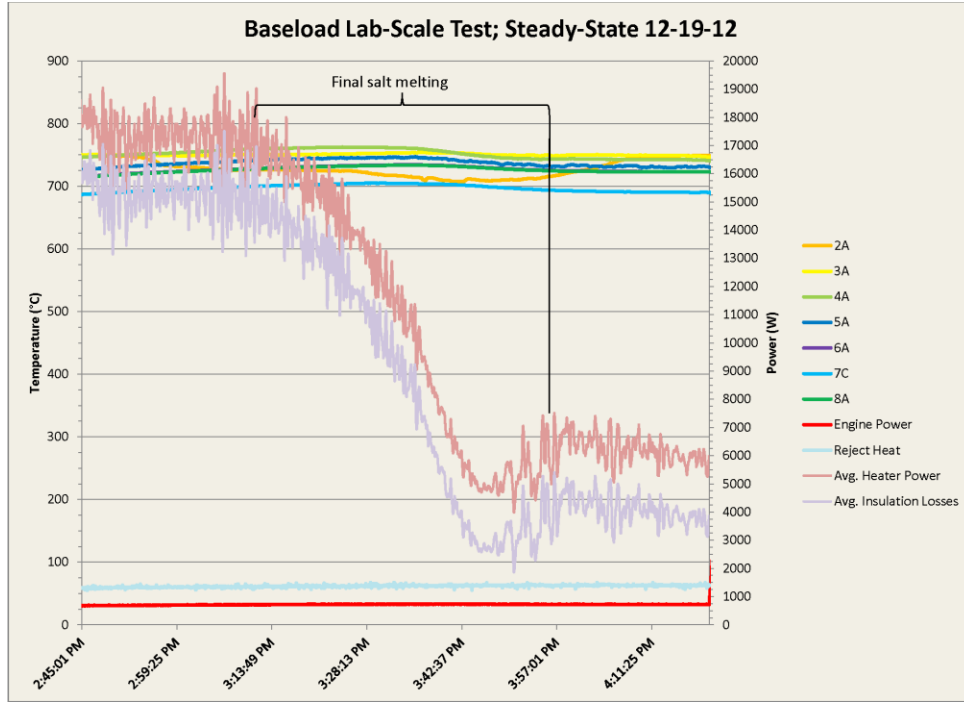


Figure 20, December 19 2012 Steady State Detail

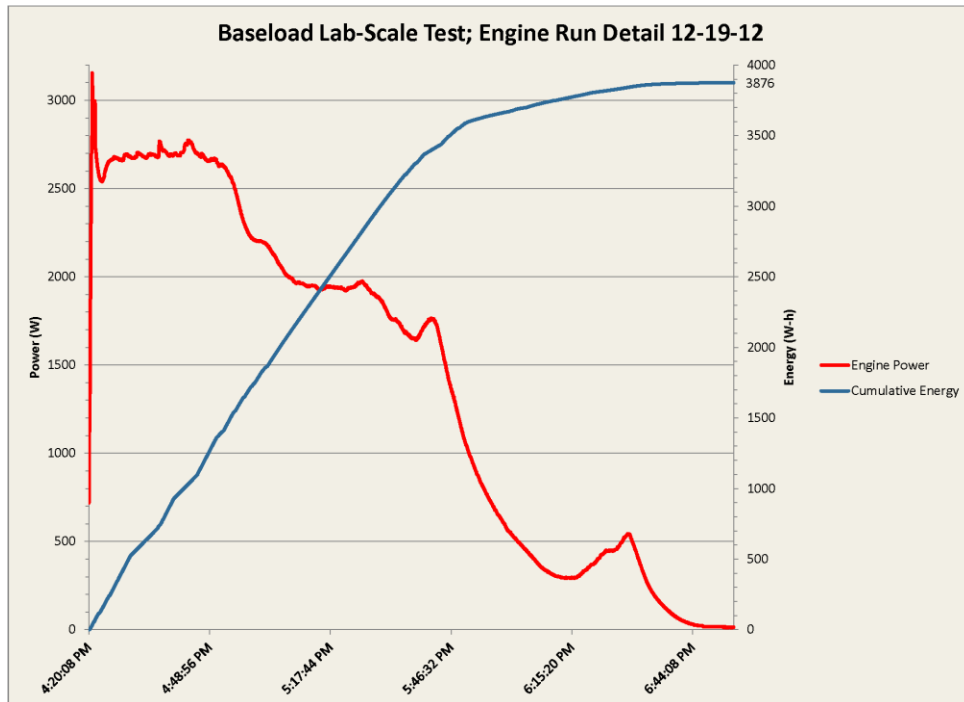


Figure 21, December 19 2012 Generator Run Detail

Task 3: Receiver/Heat Transport System (HTS)

An evaluation of pumped high-temperature heat transport systems was conducted by consultant Barry Penswick, whose report to Infinia covered extensive design and analysis of pumped loop heat transport systems to transfer heat from the solar receiver near the dish focus to the TES/engine module located on the ground. This study covered several heat transport fluid alternatives including both molten salts and liquid metals, pumped loops with and without intermediate heat exchangers (that use a secondary heat transport fluid), mechanical and electromagnetic pumps, and different TES system topologies. While the report consisted of over 20 pages of interesting and relevant assessments, the 50 page constraint for this report required relegating this task summary to conclusions only.

While a wide range of system power levels were to be considered in this evaluation, it became quickly evident that except for a few potential applications as “auxiliary” flow generation devices, the pumped HTS / TES systems were likely to be restricted to systems operating at gross power levels well above those of a single Infinia 3 kW engine system. While no specific lower bound could be specifically identified, all indications are that this type of system is more applicable to engines of 30 kW or more.

The remote location of the TES material and power conversion system from the solar receiver system has a number of very positive advantages over systems in which the 3 components are closely integrated into a single package. Of particular importance is the mounting of the TES / engine system at ground level and the ability to control the operation of the TES / engine interface more effectively during charging and discharging of the TES material in conjunction with the engine. In addition, Stirling engines have been successfully operated on pumped liquid metal loops and shown to provide excellent performance.

The primary challenging item in question is the circulating pump itself; particularly its reliability and cost at the relatively small sizes being considered.

The following items are important to consider:

- 1) Existing mechanical pumps for salts or LM heat transport system fluids are readily available for situations where the working fluid temperatures are less than about 500 to 550°C. While these pumps are currently available in higher than necessary flow rates, the basic design can be employed for lower flow rate

Innovative Phase Change Thermal Energy Storage Solution for Baseload Power
Infinia Corporation

systems. Pump operating life data is somewhat limited by the fact that existing pumps have high maintenance requirements.

- 2) It is likely that pumped loop systems will be restricted to larger installations with significant TES capacity.
- 3) Due to the significant effect of the HTF high-side temperature on the pump life and cost, it is imperative that all the heat exchangers involved with the system be as efficient as possible so as to minimize the peak fluid temperatures required to meet system power production requirements. The payoff for such a focus can be very significant in initial cost and operating life of the pump and fluid loop components.
- 4) The “hybrid” TES configuration is interesting due to its potential simplicity. However, this configuration requires that the Stirling engine portion of the system have a wide operating temperature range during TES system operation. This would require significant modification to the design of existing Infinia engines in the area of their hot end heat exchangers and would compromise efficiency.

Task 4: System Preliminary Design

At this time, the larger 3 kW_e, 12-hour storage system has not been developed. The lack of performance data with the smaller, 1-hour device precludes any efforts at a definitive system design. In addition, it is evident from the results of the heat transport system study conducted in Task 3 that pumped loop systems using liquid metals as a working fluid are limited to temperatures significantly lower than can be effectively used in the current system. The exception to this would be to use EM pumps, which are prohibitively expensive and inefficient.

One particularly attractive alternative to a dish-based design for collecting solar energy is that of using a heliostat field, whereby the TES and generator(s) are mounted at the top of a tower. This arrangement has the advantage of eliminating any pumps for transporting heat into the TES salt, as the salt can now be heated directly by the heliostat field. In addition, the TES salt and generator(s) are stationary in the preferred orientation for the salt and pool boiler – no special accommodations need be made for orientation of the TES/generator while the sun is tracked.

A small heliostat field suitable for a 30 kW system is shown in Figure 22; the solar receiver located at the top of the tower would provide direct heating to the TES vessel.

Innovative Phase Change Thermal Energy Storage Solution for Baseload Power
Infinia Corporation



Figure 22, Baseload Heliostat (Tower) Concept

Infinia believes that the tower approach is superior to the dish approach for this concept. It is envisioned that a preliminary design for a 12 hour, 3 kW_e system would be designed around a tower at the successful conclusion of the lab demonstrator.

An alternative approach to consider a heat pipe HTS between a solar receiver and the engine/TES module located behind the dish but moving with it was originally proposed as illustrated in Figure 23 on the left. The module is oriented at 45° to the dish axis so that with adequate void volume above the TES the heater head will remain above the salt surface in any orientation. This approach was not further developed in Task 4, but interest was recently rekindled by a similar mounting approach for a proposed Sandia concept from [Andraka et al, 2012] as shown at the right in Figure 23. The Sandia concept is to use a copper/silicon metal eutectic for the TES material with heat pipes to transport the heat to and from the TES module. This appeared feasible for a 25 kW engine size with 6 hours of storage, so it helped to reinforce the original Infinia approach in light of the negative conclusions for the ground mounted TES alternative. Infinia proposes to focus on this concept as the primary option for Phase II, in collaboration with Sandia for their expertise with the pumped loop heat pipe between the receiver and TES module.

Innovative Phase Change Thermal Energy Storage Solution for Baseload Power Infinia Corporation

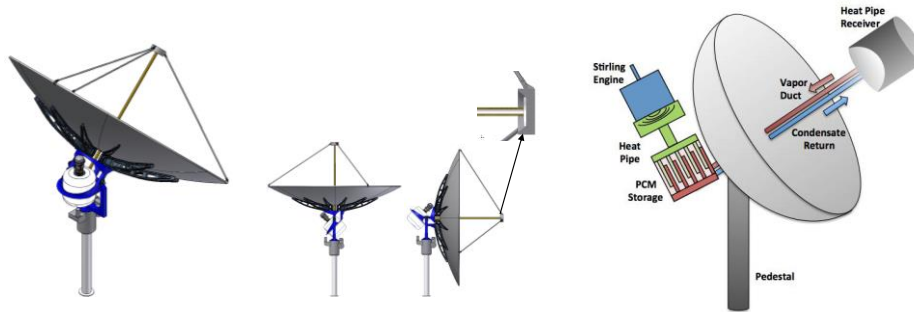


Figure 23: Originally proposed TES module behind dish (left) and recent Sandia concept (right)

Task 5: Cost and Capacity Factor Analysis

The completion of Task 5 is also interdependent on the completion of the lab demonstrator, heat transfer system, and preliminary system design tasks. Without final results of these tasks, it is not possible to conduct a detailed analysis of the costs. However, in an effort to provide an “apples-to-apples” comparison between Infinia’s TES technology and DOE’s goal of 6¢/kW-hr, Infinia has developed a preliminary LCOE analysis using a modified Solar Advisory Model (SAM).

Model Description

Infinia’s LCOE model was adapted from the Black & Veatch LCOE Model to match DOE’s LCOE reference. The model uses the same DOE LCOE equations used in NREL’s SAM model to calculate “real” LCOE values (that adjust for inflation) and “nominal” LCOE values (without adjustments for inflation). A custom TRNSYS Energy Model is used to predict system annual kWh and solves for the lowest LCOE value to meet financial metrics. The Infinia LCOE model was improved so that it is capable of matching DOE’s Tower CSP LCOE projections reference data set within 2¢/kW-hr.

Model Results

Using the modified SAM model to account for TES, Infinia compared the LCOE of three different systems, including the Colorado PowerDish, the PV Mono-Crystalline system, and the 7.5 kW Bonneville PowerDish, as shown in Figure 24. It was determined that the Bonneville PowerDish system clearly demonstrated the lowest costs per kilowatt hour. **Infinia calculated the conservative real LCOE to be 7¢/kW-h.**

Innovative Phase Change Thermal Energy Storage Solution for Baseload Power
Infinia Corporation

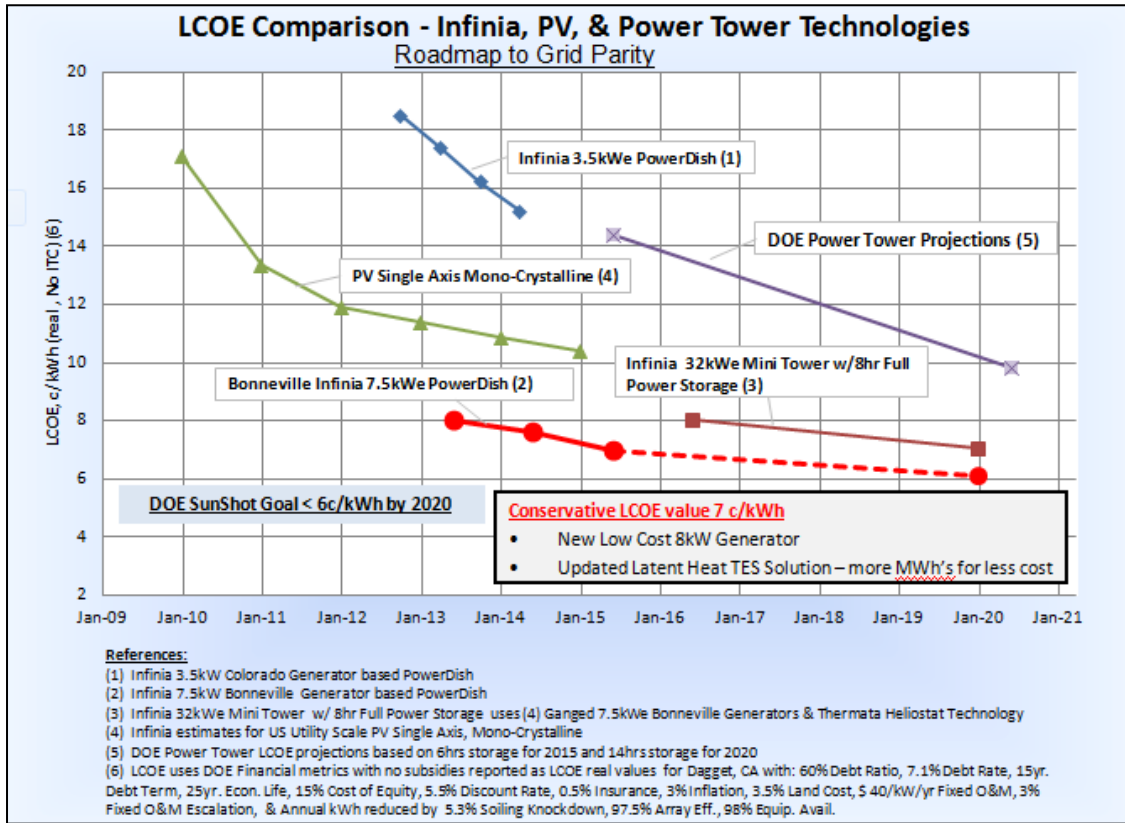


Figure 24, LCOE Comparison Graph

Additionally, a LCOE comparison of various technologies against DOE CSP financial assumptions was conducted, as shown in Figure 25. As shown in this plot, the Infinia PowerDish™ technology demonstrates one of the lowest LCOE values.

Of greater note is that the inclusion of TES within the PowerDish™ technology reduces initial costs by 20%, after which a 3% cost down with a 2% performance increase is deduced from current estimates.

Innovative Phase Change Thermal Energy Storage Solution for Baseload Power
 Infinia Corporation

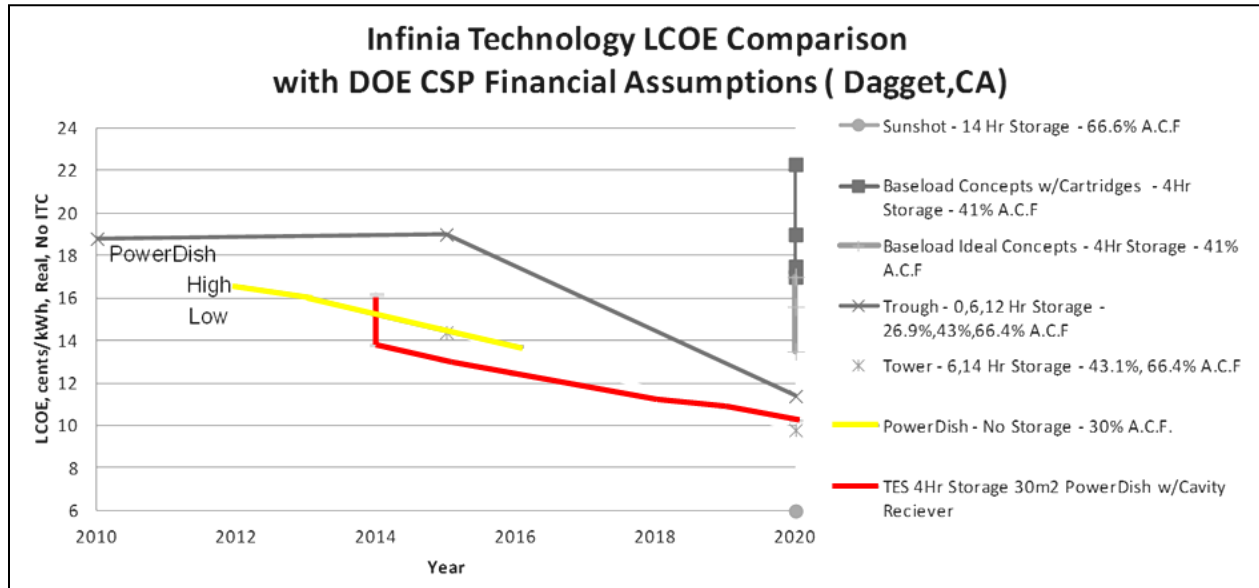


Figure 25, CSP LCOE Comparison & PowerDish LCOE With/Without TES

Conclusions: Significant delays were incurred at the outset of the project due to the efforts to validate the basic physics and functionality of the integrated TES/pool boiler concept using low cost subscale test units. Despite the delays, valuable data was collected, and the basic function confirmed. The subscale units informed key design features of the larger, lab-scale module which had a partially successful preliminary demonstration of the technology in late 2012. Initial testing exceeded by 30% the basic Phase 1 objective of 3 kW-h for net electricity produced while operating on TES stored energy only, but the output was well below the nominal generator power level. More work is needed to better understand and modify the freezing characteristics of the salt, but the energy density already exceeds that of alternative TES approaches, and the hermetically sealed system is also simpler than any known alternative.

A detailed scoping study of a heat transport system for a dish-mounted solar receiver was conducted, the conclusion of which is that the state-of-the-art for molten salt or liquid metal pumps are limited to temperatures below that which are useful for this concept. However, it has come to light that a tower-mounted TES with heliostat field has significant advantages for this system and should be considered for larger scale designs.

A preliminary design for a 3 kW_e, 12-hour storage system has not yet been developed, pending results of the lab-scale testing. However, a rough LCOE estimate for a 30 kW_e,

Innovative Phase Change Thermal Energy Storage Solution for Baseload Power
Infinia Corporation

4 hour design was conducted, resulting in a real LCOE of 13.49 ¢/kW-h. Given Infinia’s ongoing development of a high power density (7.5 kW) next generation generator and favorable scaling factors, it is anticipated that the DOE goal of 9 ¢/kW-h is still within reach for this technology.

Budget and Schedule: A summary of the project financial metrics is shown in Table 2: Project Financial Metrics.

Table 2: Project Financial Metrics

Phase	Start Date	Gov. Budget	Cost Share	Total Budget	Gov. Spent	Cost Share	Total Spent	Total Remaining
1	10/1/2010	\$999,328	\$249,832	\$1,249,160	\$999,328	\$249,832	\$999,328	\$0
2	TBD	\$999,582	\$249,896	\$1,249,478	\$0	\$0	\$0	\$1,249,478
3	TBD	\$999,962	\$999,962	\$1,999,923	\$0	\$0	\$0	\$1,999,923

Path Forward: Given what was learned in the heat transfer system scoping study about the state of the art in high temperature pumping systems and their shortcomings with respect to use in a dish-based heat transport system, it is envisioned that the path forward would entail a slight deviation from the original SOPO.

In the interim period from when the project began, Sandia National Laboratories (SNL) published a report [Andraka et al, 2012] titled “Technical Feasibility of Storage on Large Dish Stirling Systems”. In this report, the authors detail a potential configuration for a dish-mounted TES system, in which the Stirling engine and PCM storage are located behind the pivot of a mirrored concentrator. The concentrated sunlight is absorbed by a sodium heat pipe receiver at the dish focal point. The sodium vapor travels down the dish axis in a duct, where it condenses in a system of heat pipes embedded in a mass of PCM. The condensate is returned to the receiver via a separate pipe. A second set of heat pipes embedded in the PCM transfers heat to the Stirling engine.

This system is very similar to the one proposed by Infinia in the original baseload proposal. The missing piece at the time was the heat transport system from the receiver to the TES module. By combining the current TES/engine approach with the heat transport system from SNL, a complete solution for a dish-mounted Stirling system with TES can be developed. A picture of such a conceptual system is shown in Figure 26.

Innovative Phase Change Thermal Energy Storage Solution for Baseload Power
 Infinia Corporation

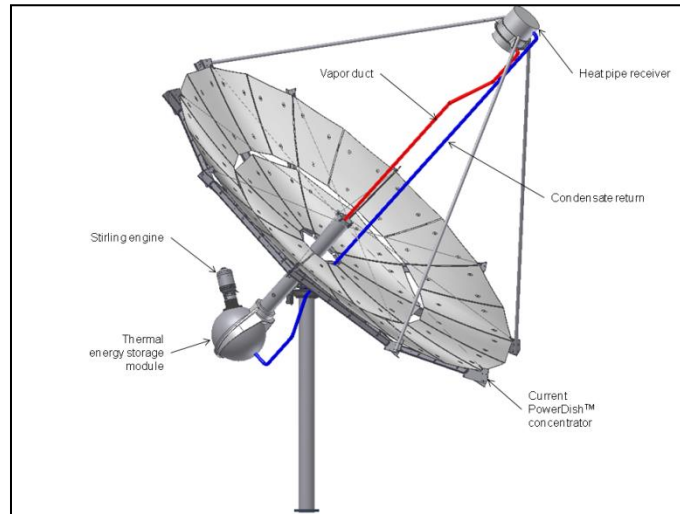


Figure 26, Dish-Mounted TES/Stirling System

The system shown uses a current generation Infinia PowerDish™ concentrator, which utilizes a “dish forward” structural approach as outlined in the SNL report. To the rear of the dish is mounted a 3 kWe Infinia free-piston Stirling engine, mated to a TES vessel. The TES/engine assembly is located behind the elevation pivot, and thus counterbalances the dish structure and receiver assembly. The engine is oriented with respect to the TES vessel such that the heater head is always above the pool boiler, regardless of whether the dish is pointed at the horizon or zenith. A duct for transporting sodium vapor to the TES is shown in red, while the condensate return from the TES back to the receiver is depicted in blue.

The TES vessel itself becomes the receiver heat pipe condenser in this scheme. This can be accomplished by adding a second shell around the primary vessel. The annular space between the inner and outer shells becomes the condenser space for the sodium vapor from the receiver. Since the space between the shells is evacuated, the inner vessel is well insulated against heat loss upon discharge. However, the outer shell must still be well insulated during charging such that the majority of the incoming energy is absorbed by the inner shell, which is in contact with the PCM.

The following is a summary of the proposed Phase 2 tasks going forward:

Task 1: TES Detailed Design - Based on the results of the Phase 1 laboratory demonstrator and the needs of the heat transport system (HTS) envisioned in Figure 26, this task will develop the detailed drawings, bill of materials (BOM) and technical

Innovative Phase Change Thermal Energy Storage Solution for Baseload Power
Infinia Corporation

specifications necessary to procure or manufacture and to assemble all component parts and subassemblies of the 3 kW_e, 12 hour TES subsystem. Based on extensive Infinia experience with a wide range of Stirling systems, this is a relatively straightforward engineering task that will be implemented using the Autodesk™ Inventor 3-D solid modeler CAD program. Any necessary integration of the TES module with both the engine and the HTS will occur under this task.

Task 2: Heat Transport System Detailed Design – The HTS would be developed in partnership with Sandia National Laboratories. SNL has extensive experience with liquid metal heat pipes and heat pipe receivers, and have demonstrated both with great success. Development here would focus on design and analysis of the spherical heat pipe absorber geometry, wicking structure and materials, vapor duct, condensate return system, and interface with the TES vessel condenser. Again, this task will develop the detailed drawings, bill of materials (BOM) and technical specifications necessary to procure or manufacture and to assemble all component parts and subassemblies of the HTS subsystem.

Task 3: Dish Detailed Design - Infinia has already developed a low-cost, dish-forward-style concentrator for the current generation PowerDish™ system. These concentrators will be deployed in a 1.5 MW field at the Tooele Army Depot in Q1 of 2013. This existing dish design will be the basis for the proposed system. Tasks will include structural and optical analysis using the anticipated loads imposed by the TES system, and optimizing the structure as needed.

Task 4: On-Sun HTS Demonstration - The HTS system design is a critical task in Phase 2. Prior to integrating it with the 3-kW baseload system in Phase 3, it is important to evaluate the operation of the selected HTS in a representative manner. The proposed approach for this is to replicate the Phase 1 lab demo unit with the addition of the double-wall vessel feature, which acts as the receiver heat pipe condenser. A solar receiver designed to interface with an existing Infinia dish will be integrated with the HTS and the engine/TES module will be mounted behind the dish as discussed earlier. The existing dish can support the on-dish options for a 1-hour TES system with minimal modifications. This will enable validation of the critical HTS approach with a low capacity factor demonstration to support the Phase 3 go/no go decision. Task 5: System Integration Final Design – This task entails integrating both the TES, HTS and concentrator system designs from Tasks 1, 2 and 3. This task is conducted subsequent to the on-sun HTS demonstration, such that any required modifications can be incorporated based on testing results. The design will be executed using the

Innovative Phase Change Thermal Energy Storage Solution for Baseload Power
Infinia Corporation

Autodesk™ Inventor 3-D solid modeler CAD package that is standard for Infinia. The final design will include all drawings and specifications needed to fabricate and assemble the full 12-hour 3-kW baseload solar power demonstration unit in Phase 3.

Task 6: LCOE/Capacity Factor Refinement - The cost and capacity factor analysis that was conducted in Phase 1 will be revisited and updated using similar approaches to those employed in Phase 1. Reasons for change include such items as feedback from vendors during TES production; TES design changes to improve performance or cost, new production candidates identified, and development of or identification of improved or lower cost processing. This information will be used to develop an updated and improved production cost assessment and revise the LCOE accordingly. Estimates for various production volumes will be completed and the direct impact of the TES engine component on overall system LCOE will be refined. In the event that cost projections are above the target values, a technology roadmap will be identified with the potential to achieve the DOE baseload power goals.

Task 7: Project Management and Reporting - Project Management will occur as a task in each phase. Task 7 will coordinate overall efforts and capture the work related to reporting, presentations, and ensuring project goals are met. Specific items derived will include a Phase 2 Final Report containing results of the subsystem and system detailed design tasks, the HTS on-sun demonstration results, an updated manufacturing cost and capacity factor analysis (including LCOE update from the SAM model), and a refined development plan for Phase 3, as well as quarterly reports, annual reports, and annual presentations.

The Tasks presented above will be completed according to the 15 month schedule shown in Table 3.

Table 3: Phase 2 Schedule

ID	Task Name	Duration	Start	Q1 '13			Q2 '13			Q3 '13			Q4 '13			Q1 '14		
				Jan	Feb	Mar	Apr	May	Jun	Jul	Aug	Sep	Oct	Nov	Dec	Jan	Feb	Mar
1	Task 1: TES Detailed Design	24 wks	Tue 1/1/13	[Task 1: TES Detailed Design]														
2	Task 2: HTS System Detailed Design	24 wks	Tue 1/1/13	[Task 2: HTS System Detailed Design]														
3	Task 3: Dish Detailed Design	20 wks	Mon 5/13/13															
4	Task 4: On-Sun HTS Demonstration	48 wks	Tue 1/1/13	[Task 4: On-Sun HTS Demonstration]														
5	Task 5: System Integration Final Design	26 wks	Mon 9/2/13															
6	Task 6: LCOE/Capacity Factor Refinement	6 wks	Mon 2/17/14															
7	Task 7: Project Management and Reporting	65 wks	Tue 1/1/13	[Task 7: Project Management and Reporting]														

Innovative Phase Change Thermal Energy Storage Solution for Baseload Power
Infinia Corporation

Critical Milestone Phase 2 Go/No-Go Criteria

In Phase 2, the critical technical question to be answered is how to move heat from the receiver to the TES/Engine. This heat transport system will be designed and demonstrated by the end of Phase 2. The HTS system must be effective in moving heat from the receiver to the TES device with high efficiency and within operational constraints. If achieved, the project will be recommended to proceed to Phase 3 for final system fabrication and demonstration. At present, this system will be based on Infinia's 3-kW concentrator with additional mirror facets added to provide the necessary added energy collection and a different structure design to support TES mass, HTS system and engine mounting.

DOE will make the ultimate decision whether a project will be entitled to proceed. DOE will also verify the economic analysis as part of the go/no go decision.

Critical Milestones for Phase 2 include:

- Fabrication of a HTS demonstration device and successful testing and evaluation on an existing Infinia dish.
- Development of a refined LCOE analysis for the TES/CSP integrated system and projected capacity factor with a levelized cost of energy (LCOE) for dish systems of 8 to 9¢/kWh, in real 2009\$, and a capacity factor of 75% (6500 hours per year of operation; at least 85% of electricity from CSP) by 2020 for a 100 MW or greater CSP power plant. A detailed cost analysis, including breakdown of component, material, and labor costs, will be submitted using the SAM model economic assumptions provided.
- Critical design review to enable DOE to evaluate the engineering design and analysis.

Phase 2 Deliverables and elapsed time after Phase 2 initiation:

- Quarterly Report #1 – 3 months
- Annual Report Input #2 for SETP Program – 3 months
- Quarterly Report #2 – 6 months
- Quarterly Report #3 – 9 months
- Fabricate HTS Demonstration Unit – 9 months
- Annual Report #1 – 12 months

Innovative Phase Change Thermal Energy Storage Solution for Baseload Power
Infinia Corporation

- Presentation #1 – 12 months
- Final Report/Final Design/Continuation #2 – 15 months

The following is a summary of the proposed Phase 3 tasks going forward:

Task 1: Fabricate/Procure all Demonstration Components - The TES, dish, HTS and balance-of-plant designs finalized in Phase 2 will be the basis for fabrication and procurement of all components and subsystems necessary for assembling the Phase 3 demonstration system. Infinia supply chain specialists will be used for sourcing fabricated items, with commercial off-the-shelf products used where possible and specialized product and service suppliers used as required.

Task 2: Assemble System - Ship all subsystems to the test site. Provide necessary support staff to assemble and install the subscale 3-kW baseload power demonstration system at SNL or an alternative location selected during Phase 2. Resolve any issues necessary to achieve successful operation on-sun and demonstrate readiness to conduct field testing.

Task 3: Test and Evaluate - Develop a comprehensive test plan to implement safe testing and operation for on-sun testing at Sandia or selected alternative site. Provide engineering and technical support staff to resolve any startup and operational issues and to address any need for functional improvements identified during testing. Conduct testing over a range of environmental and operational conditions to document the performance envelope. When any operational issues have been resolved and the basic test objectives have been achieved, delegate primary testing oversight to the staff at Sandia (or other selected site) and provide further direct support only on an as-needed basis. This will enable extensive reliability/endurance testing to be conducted during the balance of Phase 3, and beyond that if possible.

Task 4: 30-kW System Preliminary Design - The 3-kW system is considered to be a small-scale demonstration to validate the innovative concepts proposed at baseload capacity factors. To meet the target LCOE of 9¢/kWh or lower, it is anticipated that larger TES and energy conversion modules will be required. Since Infinia is developing a 7.5 kW FPSE as its next generation product, that is a natural fit for use in a commercial baseload solar product. In this regard, it is envisioned that two pairs of horizontally opposed 7.5 kW engines can be arranged in the vapor space above the TES pool boiler. Even with very conservative high allowance estimates for system capital costs, the preliminary SAM model run for Phase 1, Task 5 (Cost and Capacity

Innovative Phase Change Thermal Energy Storage Solution for Baseload Power
 Infinia Corporation

Factor Analysis) indicates that the target can be achieved. Based on all the knowledge gained from earlier phases of the project, a preliminary system design for the commercial 30-kW baseload system will be done in this task. It is clear that the required TES tank size is not consistent with a direct dish mount, so a fixed mount configuration is envisioned, probably in the form of a mini central receiver system. In this case, the engine/TES module can be placed directly on the tower for the most efficient close coupled integration of the TES with the receiver.

The close integration of the TES to the receiver allows for potentially heating the salt directly or by heating a close coupled Na heat pipe receiver or pool boiler.

Task 5: LCOE/Capacity Factor Verification – This task will confirm and finalize LCOE and capacity factor projections based on actual field data. The cost analysis that was conducted in earlier phases will be updated; including O&M cost projections, based on the latest available information.

Task 6: Project Management and Reporting - Project Management will occur as a task in each phase. Task 6 will coordinate overall efforts and capture the work related to reporting, presentations, and ensuring project goals are met. Specific items derived will include a Phase 3 Final Report containing results of the 3-kW baseload system fabrication and testing, a final revision to the manufacturing cost and capacity factor analysis (including LCOE update from the SAM model), and results of the 30-kW baseload system preliminary design, as well as quarterly reports, annual reports, and annual presentations. It is preferred that the on-sun system testing of the 3-kW baseload capacity subscale system occur at Sandia National Laboratory, However Infinia can conduct the demonstration at its facility or other selected site.

The Tasks presented above will be completed according to the 18 month schedule shown in Table 4.

Table 4: Phase 3 Schedule

ID	Task Name	Duration	Start	Finish	Q2 '14			Q3 '14			Q4 '14			Q1 '15			Q2 '15			Q3 '15		
					Mar	Apr	May	Jun	Jul	Aug	Sep	Oct	Nov	Dec	Jan	Feb	Mar	Apr	May	Jun	Jul	Aug
1	Task 1: Fabricate/Procure all Demonstration Components	36 wks	Mon 3/31/14	Fri 12/5/14	[Gantt bar spanning from Mon 3/31/14 to Fri 12/5/14]																	
2	Task 2: Assemble System	8 wks	Mon 12/8/14	Fri 1/30/15	[Gantt bar spanning from Mon 12/8/14 to Fri 1/30/15]																	
3	Task 3: Test and Evaluate	33 wks	Mon 2/2/15	Fri 9/18/15	[Gantt bar spanning from Mon 2/2/15 to Fri 9/18/15]																	
4	Task 4: 30 kW System Preliminary Design	16 wks	Mon 12/8/14	Fri 3/27/15	[Gantt bar spanning from Mon 12/8/14 to Fri 3/27/15]																	
5	Task 5: LCOE/Capacity Factor Verification	12 wks	Wed 6/24/15	Tue 9/15/15	[Gantt bar spanning from Wed 6/24/15 to Tue 9/15/15]																	
6	Task 6: Project Management and Reporting	77 wks	Mon 3/31/14	Fri 9/18/15	[Gantt bar spanning from Mon 3/31/14 to Fri 9/18/15]																	

Phase 3 Evaluation Summary/ Project Final Report Deliverables:

The Final Project Report shall contain the following:

Innovative Phase Change Thermal Energy Storage Solution for Baseload Power
Infinia Corporation

- Complete documentation of the concept/component, the design, and testing
- Updated performance cost estimates related to the capacity and cost goal
- Identification of issues and barrier and mitigation approaches
- Final capacity factor and cost of the proposed design (solar produced and total)
- Environmental impact of the approach (e.g. amount of water required, physical footprint, hazardous materials utilization, carbon emissions including the net impact from hybridization, etc.)
- Project aspects designed to mitigate environmental impact

References:

[1] DOE (2012). *Sunshot Vision Study*, retrieved on November 8, 2012.

[2] Lavinia Gabriela SOCACIU (2012). *Thermal Energy Storage with Phase Change Material*, *Leonardo Electronic Journal of Practices and Technologies*, Issue 20, January-June 2012, p. 75-98, retrieved on November 11, 2012 from <http://lejpt.academicdirect.org/A20/075_098.pdf>

[3] EPRI (2009). *Program on Technology Innovation: Evaluation of Concentrating Solar Thermal Energy Storage Systems, 1018464, Technical Update, March 2009*, retrieved November 8, 2012.

[4] IEA (2010). *Technology Roadmap: Concentrating Solar Power*, retrieved on November 8, 2012

[5] AREVA (2012). *AREVA News, Press Release on September 11, 2012 – AREVA INTEGRATES ENERGY STORAGE IN ITS SOLAR CLFR DESIGN AT SANDIA NATIONAL LABS*, retrieved on November 11, 2012 from <<http://us.aveva.com/EN/home-1977/aveva-solar-power-salt-storage.html>>

[6] IRENA (2012). *Renewable Energy Technologies: Cost Analysis Series, Volume 1: Power Sector, Issue 2/5, Concentrating Solar Power*, retrieved November 8, 2012

[7] NREL (2011). *Summary Report for Concentrating Solar Power Thermal Storage Workshop: New concepts and Materials for Thermal Energy Storage and Heat-Transfer Fluids May 20, 2011*, Technical Report, retrieved November 11, 2012 from <<http://www.nrel.gov/docs/fy11osti/52134.pdf>>

[8] Kolb, Gregory J. (2011) *An Evaluation of Possible Next-Generation High-Temperature Molten-Salt Power Towers*, Sandia National Laboratories.

Innovative Phase Change Thermal Energy Storage Solution for Baseload Power
Infinia Corporation

- [9] Atul Sharma, V.V. Tyagi, C.R. Chen, D. Buddhi (2009). *Review on thermal energy storage with phase change materials and applications*, *Renewable and Sustainable Energy Reviews* 13 (2009) 318-345, retrieved on November 11, 2012 from <<http://www.seas.upenn.edu/~meam502/project/reviewexample2.pdf>>
- [10] Wizard Power (2012). *Wizard Power Website, Technology, Energy Storage and Transport Applications*, retrieved on November 12, 2012 from <http://www.wizardpower.com.au/index.php?option=com_content&view=article&id=15&Itemid=16>
- [11] Clean Energy (2012). *Puerto Errado 2 Thermosolar Power Plant (PE2) | Case Study, Linear Fresnel Concentrating Solar Power (LFR CSP): 30 MW*, retrieved November 14, 2012 from <http://www.cleanenergyactionproject.com/CleanEnergyActionProject/CS.Puerto_Errado_2_Thermosolar_Power_Plant___Concentrating_Solar_Power_Case_Study.html>
- [12] Andraka, Charles E., Rawlingson, Scott K., and Siegel, Nate P. (2012). *Technical Feasibility of Storage on Large Dish Stirling Systems*, SANDIA REPORT, Printed September 2012
- [13] Infinia (2008). *Innovative Application of Maintenance-Free Phase-Change Thermal Energy Storage for Dish Engine Solar Power Generation*, Infinia proposal in response to DOE FOA No. DE-PS36-08GO98032, July 14, 2008.
- [14] R. Adinberg, A. Yogev, and D. Kaftori (1999). *High Temperature Thermal Storage and Experimental Study*, *M. Phys. IV, France* 9

DE-EE0003585

Innovative Phase Change Thermal Energy Storage Solution for Baseload Power
Infinia Corporation

Appendix A: Temple University Report

Final Report on the Fluid Mechanics and Heat Transfer of Pool Boiler Thermal Storage System: Numerical Simulations and Analytical Approach

Energy-releasing regime: statement of the problem

On the current stage of the project we addressed early stages of the energy-release phase. We used the commercially available FLUENT, ANSYS, and Matlab software to model different aspects of the heat transport and the motion of solid piece of salt through melted salt. The main objective of this phase is to develop a general understanding of the processes, construct numerical and analytical approaches, and specify the areas of the particular importance. Namely, we studied the appearance of the solid component on the contact line between the salt and sodium, the sinking of the continuously solidifying pieces down to the bottom and the flows appearing in the process of sinking.

At the beginning of the energy-release regime, the salt is in the liquid phase. However, as the temperature drops due to heat transfer from salt to Sodium, the solidification of salt starts at the top of the salt layer, right at the salt-sodium contact plane. The energy-exchange properties depend on the motion of the solidified pieces of salt and the structure of large-scale flows. In the very beginning of the energy-release regime, the solidification happens right on the contact plane. The surface tension of the molten salt supports the solidified pieces of salt at the contact plane, just like a needle may stay on the surface of the water. The solidified piece, thus, stays in contact with the relatively cold sodium longer and gets correspondingly larger. However, at some moment the solidified piece of salt gets heavy enough that surface tension cannot compensate for the lack of buoyancy and the piece starts sinking. We performed the Numerical simulations to describe the process of solidification and showed that the surface tension forces and the uniformity of the negative heat flux's distribution play the key role in the defining the shape of solid phase. The main results of the solidification modeling are presented in the section below.

Once the shape of the solidified pellet is obtained, its dynamics in the process of sinking can be computed numerically and estimated analytically. We showed that the shape of a pellet plays the most critical role of the sinking dynamics, the time of sinking, the depth and, most importantly, on the overall heat exchange.

Main results:

Growth of solid salt on top of molten salt

density (kg/m ³) (Solid/Liquid)	1880	
Cp (J/kgK)	977	
viscosity (N/sm ²)	0.00103	
Thermal Conductivity	Phase	k (W/mk)
	Solid	4.85
	Liquid	0.74
Pure Solvent Melting Heat (J/kg)	100000	
Solidus/Liquidus Temperature (K)	960	
Liquid Temperature (K)	990	
Solid Pellet Temperature (K)	959	
Surface Tension (N/m ²)	0.073	

Notes:
similar to water
Same as NaCl from report probably low Temperature at which a phase change occurs

We performed a set of simulations to determine the role of the surface tension and distribution of the negative heat flux. All the simulations we performed in 2D, as the axisymmetric geometry was assumed. The system has dimensions of 12 mm x 20 mm (length x height). The walls (assumed to be made of aluminum) were set to have temperatures slightly above the melting temperature of the salt, 962K. This ensured that solidification did not occur on the wall and therefore no forces acting between the wall and the solid walls have to be computed.

If the uniform negative heat flux (chosen to be 30 kW/m², which is a typical value in an experimental setup) was removed from everywhere at the top of the system, then the solidification occurs uniformly across the top of the salt. This does not lead to certain thicker areas of a solid, and results in a large solid mass, that covers almost the entire domain. The depth of this solid mass depends on the time allowed for the heat flux to pull energy from the system. Characteristic results of the corresponding Fluent simulations are presented in Figure 1.

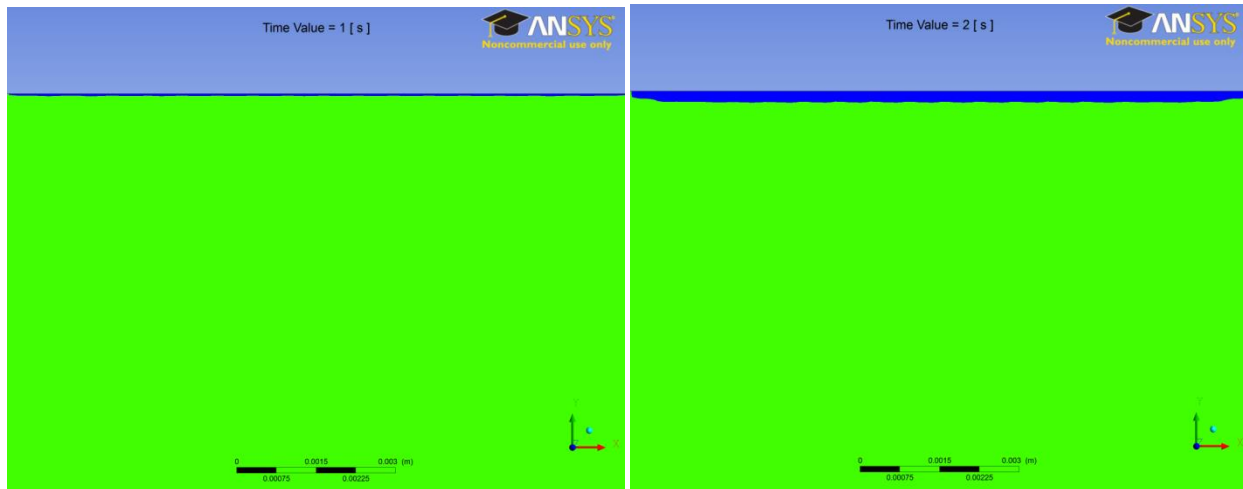


Figure 1. The solidification process in the presence of a uniform heat flux. The blue section is the solid mass, while the green is the fluid region.

If the solid layer breaks, because it is so thin, it will not travel down very far, no more than a few millimeters (see the simulations below). This will result in almost negligible large scale heat flux when compared to the heat flux that is occurring directly above it.

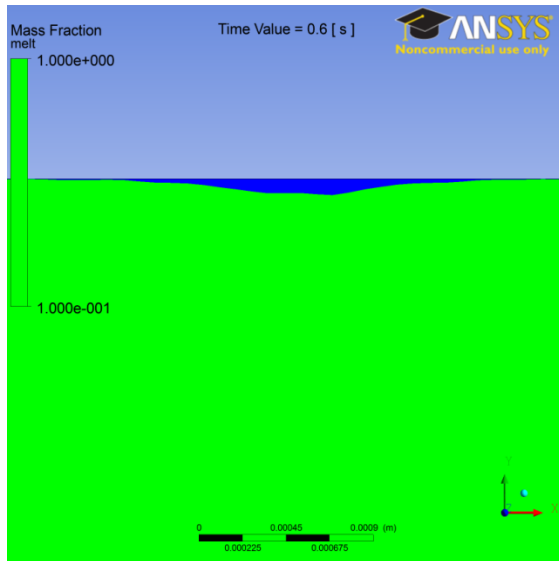
In any thermodynamical system there is always some level of fluctuation in the heat flux. We modeled several different scenarios of solidification to show what type of solid geometries would form.

In the first non-uniform scenario, we applied a uniform heat flux, but changed the initial temperature of a 1 mm section across the top to below the melting temperature. This fluctuation in temperature profile acted as a seeding point for the solidification. This scenario also resulted in a thin layer if given enough time, but before that a different geometry could form. Instead of being thin and long, the solidified mass would be thin and more localized. The size was 2.58 mm x 0.005 mm, having a slight curvature (with a length of 2.59 mm). This would be thought to be negligible, but at these dimensions the solid mass would be of sufficient size as to break the surface tension of the molten solid.

The Bond number is a dimensionless number that expresses the ratio between gravitational forces and surface tension forces. If M is the mass of the pellet, g is gravity, L is the perimeter length of the mass, and α be the surface tension value of the liquid, then the Bond number can be represented as

$$Bo = \frac{Mg}{\alpha L}, \quad \text{in 3 dimensions}$$

$$Bo = \frac{\rho g L^2}{\alpha}, \quad \text{in 2 dimensions.}$$



If the Bond number is greater than 1, then the fluid below cannot support the solid and it will break the surface and begin to sink. The geometry described above would reach a value of Bond Number above 1, so it would begin to sink. However, in this case the pellet is still a thin solid, so it would melt quickly and its descent would not span much distance before it was melted completely.

Figure 2. A solid pellet that was formed due to a 1mm-long temperature fluctuation across the top of the salt. The pellet would sink as the Bond Number becomes larger than 1.

The second scenario was to assume that the heat flux across the top was uniform in all areas except for some small distance. Instead of placing the uniform heat flux across the top of the whole domain, the extra heat flux was placed across a small span. The intervals of fluctuations were assumed to be 1 and 2 mm across – and those two values produced quite different results. The sizes were calculated until the Bond number became greater than 1, at which moment the solid mass started to sink. One can see that a large interval of fluctuations resulted in a much thinner pellet, which, as follows from the discussion presented below, is not quite effective for the heat transport down the molten salt.

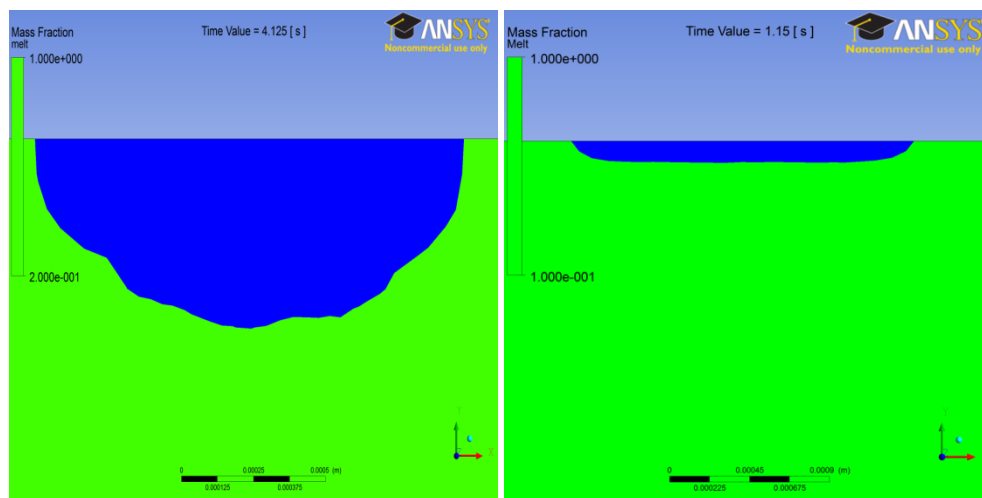


Figure 3. The solidified pellets for non-uniform negative heat flux applied over different intervals: 1mm (the left panel) 2mm (the right panel). One can see that a shorter length of the heat flux fluctuation leads to much thicker pellet .

Table 1 compares geometric values of the two reference frame trials.

Flux Length [mm]	Perimeter Length [mm]	Length Across top of Solid [mm]	Depth [mm]	Bond Number before sinking	Time of solidification [s]
2.00	1.999	2.667	0.115	1.01	1.15
1.00	2.024	1.41	0.705	1.035	2

Sinking of a solid pellet

We performed numerical simulations and analytical estimation of the dynamics of a falling solid pellet. We started numerical simulations with the shallower of the two previously discussed geometries, which corresponded to the 2mm heat flux fluctuation. This was modeled as a half- ellipsoid or a slice of a sphere, which is a close approximation of the shape found from the solidification simulation.

For these simulations it is assumed that the fluid temperature is 990k while the solid temperature is set to 959K. The rest of the parameters are the same as in the solidification simulation. The descent of the solid mass was modeled using Fluent six degree of freedom (6DOF) solver. This is compared with the reference simulation where solid mass was stationary in space and allowed to melt.

The purpose of this simulation is to see how the solid mass will melt if it did not move. This should give an order of magnitude to compare the falling pellet with. The stationary melting should be slightly longer to become completely liquid as the heat transfer into this solid will be less than if the pellet was falling. The left hand side will show the melting process of the solid mass, while the right side will show the corresponding temperature profile at that time step. The stationary solid mass takes slightly longer than 0.09 seconds to completely melt for the given conditions.

Analytical Study

Problem Description and Assumptions

Consider a pellet of salt at temperature T_1 (lower than melting point T_m) formed on the surface of a tank of melted salt due to the solidification as the heat is being pumped out from the top of the tank. Eventually the pellet starts falling down, once the surface tension of liquid salt is not able to hold it on surface. In the process of sinking the pellet melts. The goal here is to establish a model to describe the falling and melting process of the pellet through liquid salt. We are interested in the distance that the pellet travels till it completely melts.

Currently we assume that the temperature of the fluid is uniformly T_h ($T_h > T_m$) across the tank. Different temperature profiles were preliminary considered and did not seem to drastically change the dynamics. We also assume that the melting of a single pellet does not affect the temperature distribution of fluid, because of small size of pellets (characteristic size is of order of 1mm). The falling process of multiple pellets will be studied in our future work. According to the FLUENT simulation, it is reasonable to assume that the shape of the pellet is a spherical cap:

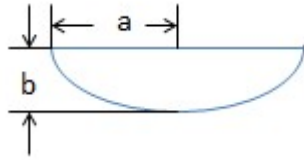


Figure 4 A 2D view of the spherical cap.

The radius of the sphere (R) the cap belongs to, the surface area of the curved part (S), and the volume (V) of the cap are given by:

$$R = \frac{a^2 + b^2}{2b}, \quad S = \pi(a^2 + b^2), \quad V = \frac{\pi b(3a^2 + b^2)}{6} \quad (1)$$

Based on the observations from the numerical simulations, the melting is much more intensive at the upfront of the cap. So the heat convection through the back of the cap is neglected in current model.

Main Equations

In order to establish the equations of the model, we introduce a set of variables which are dependent of time t during the falling and melting process:

$$q = D, u, a, b \quad (2)$$

where D is the distance traveled by a pellet, u is the velocity, a is the radius of the circular back, and b is the height of the cap, respectively ($a \geq b$). Taking derivative of Eq.2} with respect to t we obtain

$$q = \dot{D}, \dot{u}, \dot{a}, \dot{b} \quad (3)$$

Where \dot{D} is the velocity, \dot{u} is the acceleration, \dot{a} and \dot{b} is the rate of change of a and b respectively. One can see that $\dot{a} = \frac{R}{a} \dot{b}$.

By definition of velocity and acceleration, the first term in Eq. 3

$$\dot{D} = u. \quad (4)$$

and the second term is

$$\dot{u} = \frac{\Sigma F}{m} = \frac{F_g - F_b - F_d}{m} \quad (5)$$

In which m denotes the mass of the pellet, F_g denotes the gravitational force, F_b denotes buoyancy, and F_d denotes the drag due to fluid viscosity. In the current study, F_d is approximated by the Stokes' drag, $F_d = 6\pi\mu u$, where μ is the dynamical viscosity of the fluid. Together with the expression of volume in Eq. 1, the acceleration can be written as:

$$u = \left(1 - \frac{\rho_f}{\rho_s}\right)g - \frac{36\mu au}{\rho_s b(3a^2 + b^2)} \quad (6)$$

where ρ_f and ρ_s are the density of the fluid and solid respectively.

The \dot{a} and \dot{b} terms are defined by the heat convection from fluid to solid as well as melting. In order to obtain an expression for these two terms, the heat transfer coefficient through a spherical surface is evaluated using the Ranz-Marshall equation with the characteristic length scale being $2a$:

$$h = \left(2 + 0.6\sqrt{Re}(Pr)^{\frac{1}{3}}\right) \frac{k}{2a} \quad (7)$$

where $Re = \frac{2\rho_f au}{\mu}$ is the Reynolds number and $Pr = \frac{C_p \mu}{k}$ is the Prandtl number. Constants k and C_p are the heat conductivity and heat capacity of the fluid.

The heat that is transferred from the fluid into the solid pellet is used for bringing the solid temperature up to melting point and then melting. Thus the heat flux can be described as:

$$(T_h - T_l)hA = \frac{d}{dt}(C(T_m - T_l)\Delta V) + \frac{d}{dt}(L_h \rho_s \Delta V),$$

where C is the volumetric heat capacity of the solid, L_h is the latent heat and ΔV is the instantaneous change in volume. Plugging in the expressions of surface area and volume yield:

$$(T_h - T_l)h\pi(a^2 + b^2) = -\frac{\pi}{6}(C(T_m - T_l) + L_h \rho_s)((3a^2 + b^2)\dot{b} + b(6a\dot{a} + 2b\dot{b})),$$

Taking into account that $\dot{a} = \frac{R}{a}\dot{b}$ and the definition of R given in Eq. 1, the above equation leads to:

$$\begin{aligned} \dot{b} &= -\frac{(T_h - T_l)h(a^2 + b^2)}{(C(T_m - T_l) + L_h \rho_s)(a^2 + b^2 + 2bR)} \\ &= -\frac{(T_h - T_l)h}{(C(T_m - T_l) + L_h \rho_s)}. \end{aligned}$$

Thus, Eq. 3 becomes a closed system of 4 ODEs with 4 time-dependent variables:

$$\dot{q} = \begin{cases} \dot{D} = u \\ \dot{u} = \left(1 - \frac{\rho_f}{\rho_s}\right)g - \frac{36\mu\alpha u}{\rho_s b(3a^2 + b^2)} \\ \dot{\alpha} = \frac{R}{a}b \\ \dot{b} = -\frac{(T_h - T_l)h}{(C(T_m - T_l) + L_h \rho_s)} \end{cases} \quad (8)$$

With $h = h(a, u)$ given in Eq. 7.

Non-dimensionalization

For the non-dimensionalization of the equations in Eq. 8, we chose the characteristic length scale as a_0 , which is the initial radius of the circular back of the pellet.

Introduce the following parameters:

$$a = a_0\alpha, \quad b = a_0\beta, \quad D = a_0D', \quad u = Uu', \quad h = h_0\varepsilon, \quad h_0 = \frac{k}{a_0}, \quad U = \sqrt{ga_0}, \quad t = \frac{a_0}{U}\tau.$$

Where $\alpha, \beta, D', \varepsilon, \tau$, and u' are non-dimensional radius, height, distance traveled, the heat transfer coefficient, the time, and the velocity of the pellet respectively; U and h_0 are the characteristic velocity and the heat transfer coefficient, respectively. Note that $\beta \leq \alpha \leq 1$, and $\beta = \alpha = 1$ represents a hemispherical pellet.

In terms of the new variables and omitting primes from variables we have:

$$\dot{q} = \begin{cases} \dot{D} = u \\ \dot{u} = C_1 + C_2 \frac{\alpha u}{\beta(3\alpha^2 + \beta^2)} \\ \dot{\alpha} = C_3 \frac{(\alpha^2 + \beta^2)^{\frac{1}{3}} + 0.3\sqrt{Re_0}(Pr)^{\frac{1}{3}}\sqrt{\frac{u}{\alpha}}}{2\alpha\beta} \\ \dot{\beta} = C_3 \left(\frac{1}{\alpha} + 0.3\sqrt{Re_0}(Pr)^{\frac{1}{3}}\sqrt{\frac{u}{\alpha}}\right) \end{cases} \quad (9)$$

Notice that $Re_0 = \frac{2\rho_f a_0 U}{\mu}$ is not a standard Reynolds number, as U is not a characteristic velocity of a pellet. The non-dimensional parameters C_1 , C_2 , and C_3 are

$$\begin{aligned} C_1 &= 1 - \frac{\rho_f}{\rho_s}, \\ C_2 &= \frac{36\mu}{\rho_s a_0 U} = -\frac{72(1 - C_1)}{Re_0}, \\ C_3 &= -\frac{2(T_h - T_l)h_0}{(C(T_m - T_l) + L_h \rho_s)U}. \end{aligned} \quad (10)$$

Thus, we obtained a non-dimensional system of equations, which we integrated using the Runge-Kutta method. Typical results are presented in the next section for typical values of the parameters.

Results

To test our model, we used the following value of the parameters and thermal properties, based on the material properties and reasonable assumptions: $\rho_f = 1880 \text{ kg/m}^3$, $\rho_s = 1.3\rho_f$, $L_h = 10^5 \text{ J/kg}$,

$\mu = 0.0005 \text{ N s/m}^2$, $g = 9.8 \text{ m/s}^2$, $k = 0.74 \frac{\text{W}}{\text{mK}}$, $T_l = 959\text{K}$, $T_m = 960\text{K}$, $C_p = 977 \frac{\text{J}}{\text{kgK}}$, $C = 880 \rho_s \frac{\text{J}}{\text{m}^3\text{K}}$. The non-dimensional parameter C_1 is always constant for a fixed density ratio. For considered value of parameters, $C_1 = 0.2308$. And for a typical range of the pellet radius, $0.5 \leq a_0 \leq 3\text{mm}$, we have $-0.2103 \leq C_2 \leq -0.0143$ and $-0.0053 \leq C_3 \leq -3.618e - 4$. We present typical solutions of Eq. 9 in the following figures.

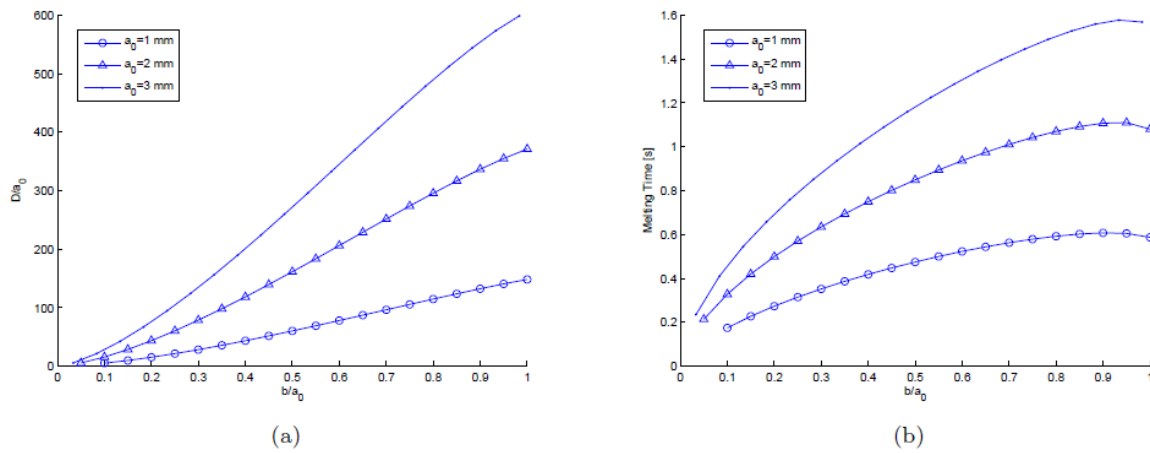


Figure 5 Dynamics of pellets in the shape of a spherical cap with initial top $a_0 = 1\text{mm}$, 2mm , and 3mm . Left: Falling distance vs. cap height. Right: Melting time vs. cap height.

To illustrate the transport of a pellet in the real space, we returned to the dimensional variables. Moreover, the falling distance and the velocity of the pellet during the falling process are presented for three typical initial pellet heights (b_0):

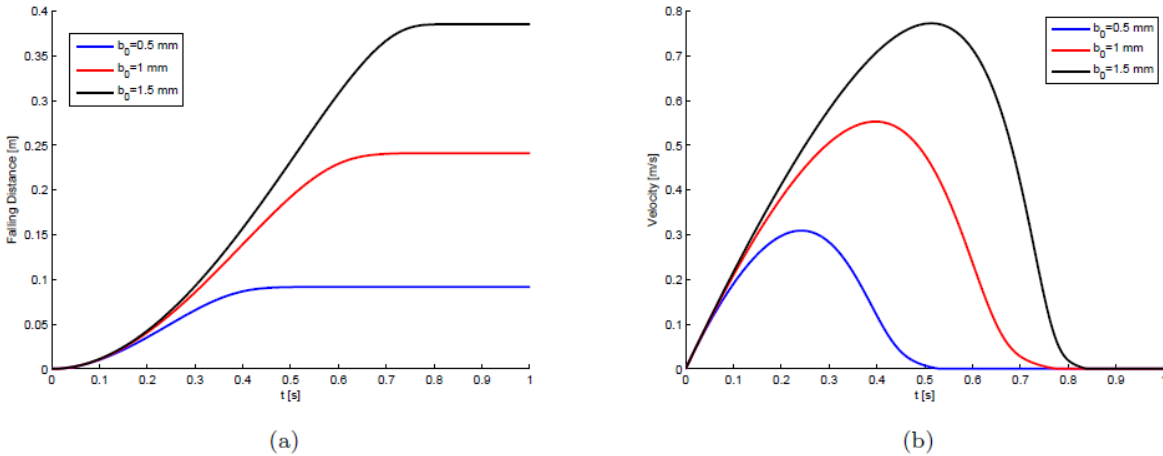


Figure 6 Falling distance and velocity evolution for a pellet of $a_0 = 1.5\text{mm}$ with $b_0 = 0.5\text{mm}$ (blue); 1mm (red); 1.5mm (black), respectively. Left: Falling distance vs. time. Right: Velocity vs. time.

Notice that in Fig. 6(a), the flat regions represent the time when the pellet has completely melted, which correspond to the regions where the velocity vanishes in Fig. 6(b). In other words, the horizontal intervals correspond to the pellet of the almost vanishing size. As shown in Fig. 6(b), the pellet initially accelerates due to the gravity, and then rapidly decelerates as the drag force acting on the pellet gets significant. During the deceleration period, the pellet reaches the instantaneous terminal velocity, which is a function of the instantaneous size of the pellet. As the instantaneous terminal velocity drops as the size of the pellet decreases, the pellet experiences a rapid decrease in velocity.

Numerical Simulations

We started numerical simulations with the shallower of the two previously discussed geometries, which corresponded to the 2mm heat flux fluctuation. This was modeled as a half- ellipsoid or a slice of a sphere, which is a close approximation of the shape found from the solidification simulation.

For these simulations it is assumed that the fluid temperature is 990k while the solid temperature is set to 959K. The rest of the parameters are the same as in the solidification simulation. The descent of the solid mass was modeled using Fluent six degree of freedom (6DOF) solver. This is compared with the reference simulation where solid mass was stationary in space and allowed to melt.

The purpose of this simulation is to see how the solid mass will melt if it did not move. This should give an order of magnitude to compare the falling pellet with. The stationary melting should be slightly longer to become completely liquid as the heat transfer into this solid will be less than if the pellet was falling. The left hand side will show the melting process of the solid mass, while the right side will show the corresponding temperature profile at that time step. The stationary solid mass takes slightly longer than 0.09 seconds to completely melt for the given conditions.

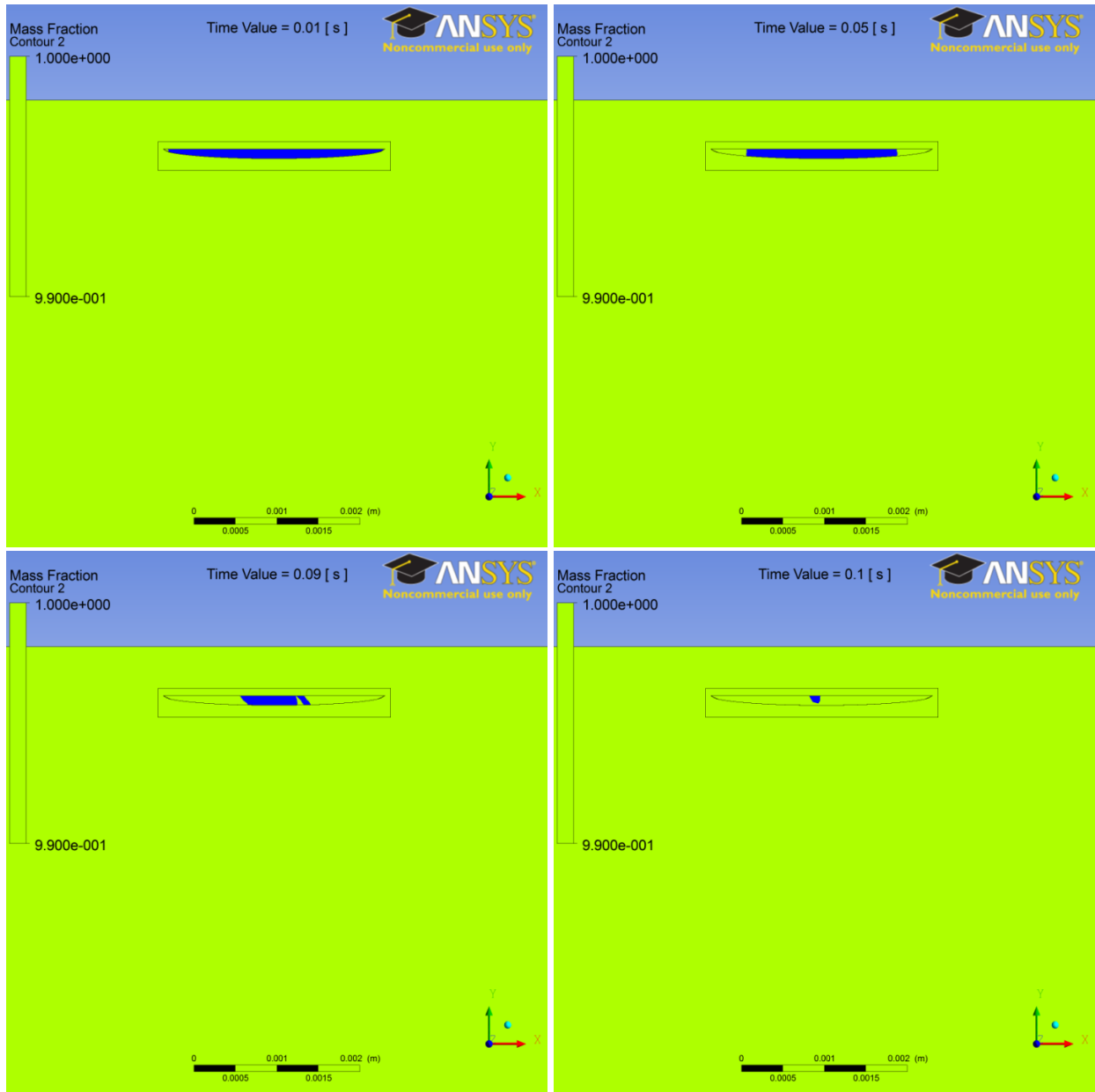


Figure 7 The shape of the solid mass while it is melting. By 0.10 seconds the stationary pellet is almost completely melted.

Melting of the falling solid mass is illustrated below and in the attached movie (falling.wmv). The green area is liquid, while the blue area is the solid mass. It is assumed that the pellet does not break up during the fall and it is treated as a bulk mass until completely melted.

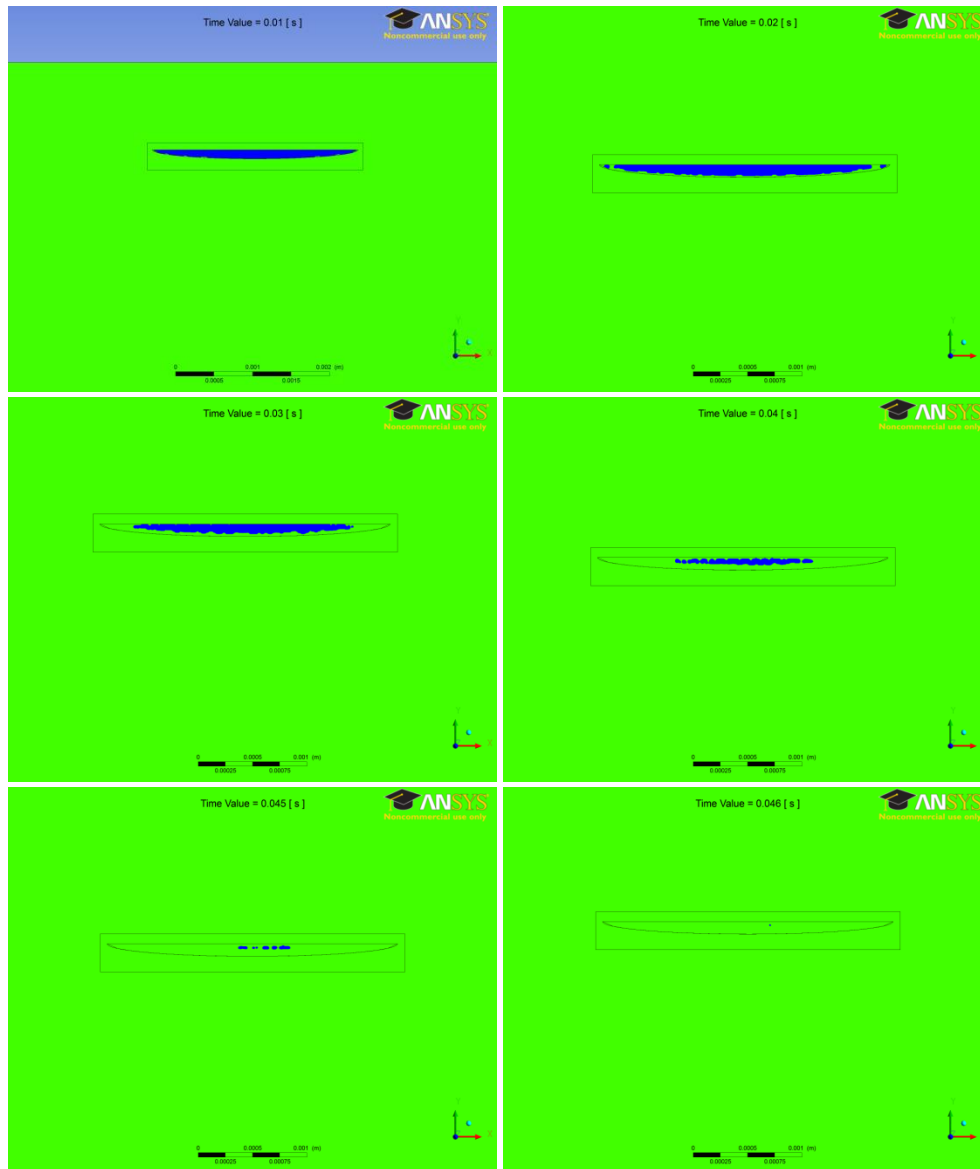


Figure 8 Melting of a falling solid pellet. The green region represents a liquid region, while the blue region is the solid mass. After 0.046 seconds the entirety of the pellet is melted.

The solid mass is completely melted by 0.046 seconds for the given conditions. This is 30% quicker than if the pellet was stationary, as is expected. From a qualitative perspective it should be noted that the temperature profile does not affect as large of an area when compared to the stationary pellet.

Summary and Discussions

During the current stage of the project, we investigated the initial phase of the energy-release process. The comparison between numerical simulations and the analytical model show quite a good agreement.

There are quite a few assumptions that were built in the analytical approach, and, thus, it is not surprising that there are some discrepancies. We assumed that the temperature of the fluid is uniform across the tank. Different temperature profiles were preliminary considered and did not seem to drastically change the dynamics.

Our preliminary results indicate that the strength of the wake first increases with the depth travelled by the pellet, as the pellet picks up the velocity, however after a certain time the size of a pellet significantly diminishes, and so does the size and intensity of the wake.

The role of the wake is two-fold. First, the advection creates an effective mechanism of intense heat exchange. Second, it creates effective perturbation of the contact plane. As a result, the solidifying pieces may be removed from the contact plane with smaller size, compared with the case of the absence of large-scale perturbations discussed above. As a result, once starting sinking, they will get re-molten faster and reducing the transport of the heat. Finally, when the number of simultaneously solidifying pieces becomes large, the advection makes it necessary to include the mutual interaction of falling pellets.

However, as the overall temperature falls, the solid pieces will be able to travel further and further down. It will result in the appearance of the flow inside the flow domain. And finally the solid pieces will start sinking all the way to the bottom.